ELECTROSPUN NANOFIBER BASED BIOSESNOR FOR ULTRASENSITIVE PROTEIN DETECTION

A Thesis by

Md. Rajib Anwar

Bachelor of Science, Bangladesh University of Engr. & Tech., 2006

Submitted to the Department of Mechanical Engineering
and the faculty of the Graduate School of
Wichita State University
in partial fulfillment of
the requirements for the degree of
Master of Science

July 2011

ELECTROSPUN NANOFIBER BASED BIOSESNOR FOR ULTRASENSITIVE PROTEIN DETECTION

The following faculty members have examined the final copy of this thesis for form and content, and recommend that it be accepted in partial fulfillment of the requirement for the degree of Master of Science with a Major in Mechanical Engineering.

_____
Ramazan Asmatulu, Committee Chair

_____
Shalini Prasad, Committee Member

_____
Hamid Lankarani, Committee Member

DEDICATION

To my family and friends

ACKNOWLEDGEMENTS

I would like to thank my advisor, Dr. Ramazan Asmatulu for his continuous support and encouragement throughout my Master's Degree. I would like to express my sincere gratitude to my committee member and co-advisor, Dr. Shalini Prasad for her guidance and support in conducting the experiments and completing the research.

My heartfelt appreciation goes to member of my thesis committee, Dr. Hamid Lankarani, for his valuable comments and suggestions on this project. I am also very thankful to Dr. Krishna K. Krishnan for giving me the chance to work with him in research project.

Special thanks go to Farhana Abedin for being such a loving wife, wonderful friend and a very supportive colleague. She helped me in conducting all the experimental works and always encouraged me in getting everything done at right time.

I would like to acknowledge Dr. Krishna Vatipalli for his help and co-operation in this work. I would like to thank all my friends and family members for their support and encouragement.

ABSTRACT

This research attempted to develop “label-free” biosensor for the detection of cardiovascular risk biomarker, C-reactive protein (CRP). An electrospun Polystyrene (PS)/ Polyaniline (PANI) nanofiber was used as the sensing element of the biosensor and coupled with electrical measurement system. High aspect ratio and porosity of nanoscale fiber provides size matched confinement for tiny biomolecule immobilization, which leads to rapid transduction and enhancement in signal strength. Nanofiber mat was integrated with a gold microelectrode interdigitated chip and microfluidic chamber to create a lab-on-chip platform.

Results demonstrated that nanotextured fiber with appropriate chemical and electrical functionality can be used as sensing element of an electrochemical biosensor for detection of biomolecules at very low concentration. CRP was successfully detected at 100 fg/ml concentration from human serum suggesting the potential of this lab-on-chip platform for early detection of any cardiovascular risk. A large dynamic linear range of 100 fg/ml-1 μg/ml was achieved in human serum for detection of CRP. Less than 10% cross-reactivity with human albumin suggests the selective detection capability of the proposed biosensor.

TABLE OF CONTENTS

TABLE OF CONTENTS (continued)

TABLE OF CONTENTS (continued)

LIST OF TABLES

LIST OF FIGURES

LIST OF FIGURES (continued)

NOMENCLATURE

PS	Polystyrene
PANI	Polyaniline
HCSA	Camphorsulfonic Acid
PPy	Polypyrrole
EIS	Electrochemical Impedance Spectroscopy
CRP	C-reactive Protein
ELISA	Enzyme Linked Immunoassay
POCT	Point of Care Testing
LOD	Limit of Detection
PDMS	Polydimethylsiloxane
MEA	Microelectrode Array
SPR	Surface Plasmon Resonance
LSPR	Localized Surface Plasmon Resonance
SAW	Surface Acoustic Wave
SERS	Surface Enhanced Raman Scattering
QCM	Quartz Crystal Microbalance

LIST OF SYMBOLS

μm	Micrometer
nm	Nanometer
ml	Milliliter
fg	Femto-gram
pg	Pico-gram
ng	nano-gram
μg	Micro-gram
°	Degree
C	Celsius
kV	Kilovolt
Hz	hertz
kHz	Kilohertz

CHAPTER 1

INTRODUCTION

1.1 Background

Sensors are devices that respond to a stimulus by providing a functionally linked response. When exposed to a quantity or parameter or an environment (measurand), it converts one or more of its properties such as optical, electrical, mass etc. in the form of a measurable signal that carries information about the measurand. The word sensor has a Latin origin. It was derived from a Latin word “sentire” which means to perceive. Sensors are all around us although many of us might not notice. Some common examples of sensors are room temperature controllers which allow the air conditioning system to maintain a constant temperature or smoke detectors that detect presence of smoke or automatic lights that turns on automatically by sensing the presence of an object. Sensors allow us to monitor our surroundings and act accordingly. Parameters that can be monitored by using a sensor include volume, temperature, humidity, pressure, vibration, fluid flow, position etc. In recent years, development of sensors has become very important. With the massive improvement of automation and electronics, sensors can be found everywhere. Large manufacturing and process industries rely heavily on sensors to remotely monitor their production process for optimized plant performance, centralized control and equipment health diagnostics. All the modern cars that we ride, the insanely amazing Boeing 787 or a space shuttle operating thousands of miles away from earth are riddled with sensors for monitoring speed, position or performance. Application of sensors can also be found in healthcare and medical diagnostics, as well as in defense applications. Sensor technology is thriving as the need for recognizing complex chemical, biological or physical phenomena and getting a quantitative measure of these systems are escalating. Sensor technology is most

probably the area where micro/nanotechnology has its utmost impact. Devices are getting smarter, smaller and cheaper every day. With the progression of micro and nanotechnology, the research focus has primarily shifted towards miniaturization. A small engineered system require fewer raw materials to produce, wastes less raw materials, consumes less power and add multifunctionality to the product. Truly multifunctional devices like i-phones are reality today because of miniaturization. We are almost at the touchline of so called top-down-approach of product manufacturing technology and the future is for bottom-up technologies. Electronic devices are soon going to reach the limit of scaling down. But nanotechnology holds a great promise to us. The future may well belong to molecular scale electronics, multifunctional nanomaterials and quantum computation. Smart, multifunctional devices with self healing systems might soon be transformed from laboratory inventions to marketable products which will make our life safer and better. The incessant quests of researchers in understanding fundamental building blocks of materials have provided us with the power to manipulate and control material in the atomic and sub-atomic level. Therefore, there is plenty of room for improvement and development in sensor technology.

Biosensors are specific type of sensors that are designed to detect any biological phenomena. A very common example of a biosensor is the glucose meter which allows us to track the blood sugar level of diabetes patients. Biosensors have become integral part of healthcare and environmental monitoring. Ability of biosensors to detect harmful pathogens and biomolecules in environment makes them a great tool against bio-warfare and terrorism. Figure 1 shows the various application areas of biosensors.

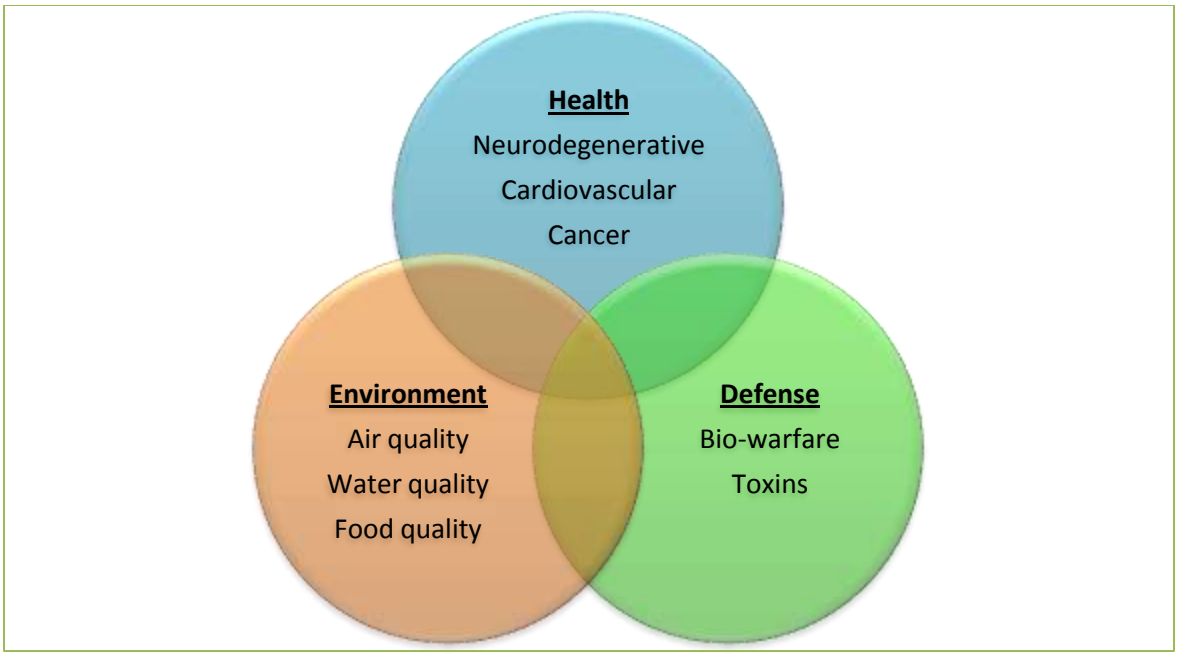

Figure 1. Different application areas of modern day biosensors.

The area of biosensor technology is quite multidisciplinary in nature. It involves knowledge derived from several traditional engineering disciplines, physics, chemistry and biology. Today, biosensor research and development is one of the most exciting fields of analytical research. With the rapid advance of nanotechnology, it is possible that nanotechnology enabled biosensors may offer significant advantages over conventional biosensors. The unique properties of nanoscale materials enable us to develop sensors with greater sensitivity, improved stability and lower power consumption.

In recent years the trend in healthcare and medical diagnostics has been towards developing personalized diagnostic devices for faster and on site diagnosis which is termed as point-of-care diagnostic testing (POCT). Early detection of disease is a key priority in health care industry. Research has been heavily focused on developing portable lab-on-chip devices for disease diagnostics and developing minimally invasive smart systems that are capable of detecting and treating human body at the earliest sight of oncoming diseases.

In this research work, electrospun nanofiber based biosensor was developed and tested for ultrasensitive protein detection. An inexpensive and smart technique was employed to fabricate nanotextured fiber mats from blend of two polymers, polystyrene and polyaniline. Smart architecture of this novel nanofiber was utilized on a gold based microelectrode platform for developing an impedimetric biosensor which has potential as a portable diagnostic device for early cardiovascular disease detection.

1.2 Scientific Motivation

The motivation for choosing a project on development of nanotechnology enabled biosensor and selecting C-reactive protein (CRP) as the model target analyte was twofold: Limitations of current diagnostic technologies and importance of early detection of cardiovascular disease.

Enzyme Linked Immunoassay (ELISA) is considered as the gold standard in current commercially available immunoassay type detection techniques. There are other techniques like immunoturbidimetry, rapid immunodiffusion and visual agglutination. Most quantitative immunoassays are based on optical detection scheme such as fluorescence or luminescence, where the presence of target analyte is quantified as a function of intensity of fluorescent signals. Currently, most disease diagnosis takes place in dedicated lab and involves bulky equipments, trained personnel and high cost. These systems have proven reliability, can detect biomarkers at clinically relevant concentrations and have high throughput of samples. However, important disadvantages of current commercial technology are associated with the requirement of having a dedicated lab, complex procedure and expensive equipment. The time between decision to test, transporting sample, getting the test done and reporting back can well be in the order of several weeks. The high therapeutic turnaround time may well become a matter of life and death.

Portable lab on chip devices can make “anytime, anywhere” diagnosis a reality where patients can be diagnosed in a matter of minutes. In some cases where routine checkup is required in low risk diseases (such as diabetes) as well as personalized diagnosis tool is required in areas where healthcare facilities are scarce, portable POCT devices can provide an alternative to dedicated diagnostic facilities and revolutionize patient experience. With the power of nanotechnology, it is possible to reduce current medical diagnosis into handheld device formats that will have high sensitivity, will require low sample volume, will be label free and will be able to detect targets real time. These nanomaterial enhanced biosensors can provide highly sensitive portable label free diagnostic device and make personalized healthcare a reality. Use of nanomaterial and electrical detection schemes has enormous potential to greatly simplify traditional technologies into POCT devices through miniaturization and cost-effective fabrication technology. This research explores the enchanting arena of nanoscale materials through fabricating electrospun polymer nanofiber and integrating it onto a lab-on-chip platform to test its performance in detection of C-reactive protein at ultra-low concentrations.

Heart disease is a major cause of death all over the world. According to “Center for Disease control and Prevention”, heart attack is the leading cause of death in USA. In 2010, an estimated 785,000 Americans had a new coronary attack and about 470,000 had a recurrent attack. The report also suggests that about every 25 seconds, an American will have a coronary event, and about one every minute will die from one. Stroke is also not far behind with 3rd position in leading cause of death. C-reactive protein is an inflammatory cardiovascular biomarker which is over-expressed when a person has a heart disease and thus early detection of CRP is vital in saving lives. The novel properties of nanoscale materials have the potential to increase the sensitivity of biosensors so that it can detect CRP at very low concentrations and

give early indication of heart problem. Being an inflammatory biomarker, CRP level also rises in case of high stress level. Therefore, the proposed portable biosensor might have probable application in on-site soldier stress level monitoring at battlefields so that corrective measures can be taken.

1.3 Specific Project Goal

The idea of nanotechnology acting as an enabler in developing highly sensitive protein detection device has been explored in this research. The specific goals of this research are listed below:

- Electrospinning polymer nanofiber mat from blend of polystyrene and polyaniline.
- Integrating nanofiber with gold microelectrode chip to create a portable biosensor for CRP detection.
- Investigating biosensor performance in quantitatively detecting CRP from both buffer and human serum.
- Bolstering the concept of nanotechnology enabled label free biosensor for portable diagnostic tool development.
- Pinpointing the limitation of proposed idea in translating it from a laboratory invention to a marketable product and open up new ventures of future research.

CHAPTER 2

REVIEW: ELECTROSPINNING AND BIOSENSOR

2.1 Electrospinning

Electrospinning, a process patented by Formhals [1] in 1934, is considered an efficient method for fabrication of nanofibers. A wide range of polymeric materials can be used for the fabrication of nanofibers. When the diameter of polymer fiber material is scaled down from micro to nano scale, several amazing and unique characteristics are observed. These fibers exhibit extremely high surface area to volume ratio, outstanding mechanical properties, high surface functionality and high porosity with exceptional pore interconnectivity. Several other methods have been used to fabricate nanoscale polymeric fibers, such as template synthesis [2, 3], drawing [4], self assembly [5, 6], phase separation [7] and melt blowing [8]. Of all these nanofiber fabrication technique, electrospinning is the easiest and fastest fabrication technique and therefore, the most promising technology for large scale production of nanofibers. The unique characteristics of electrospun nanofibers make them suitable candidate for many applications, such as composite reinforcements, filtration, smart bandages, drug delivery, tissue engineering scaffolds, implants, sensors, electronics, catalysts, affinity membranes, protective clothing, acoustic absorbing media and energy storage.

Electrospinning is mostly done in solvent solution or in melt form. The basic setup for electrospinning as shown in Figure 2, consists of a high voltage power supply, a syringe with a pipette tip or needle and a metallic collector. In electrospinning, a polymer solution is charged with high DC voltage to produce a charged jet that ejects from the pipette tip or needle. The jet travels towards a collector where it is collected as a randomly woven interconnected webs. Aligned fiber is also achievable through controlled collection process such as use of a rotating

mandrel. The solution jet evaporates or solidifies on the way to collector screen to produce thin sub-micron size polymeric fibers.

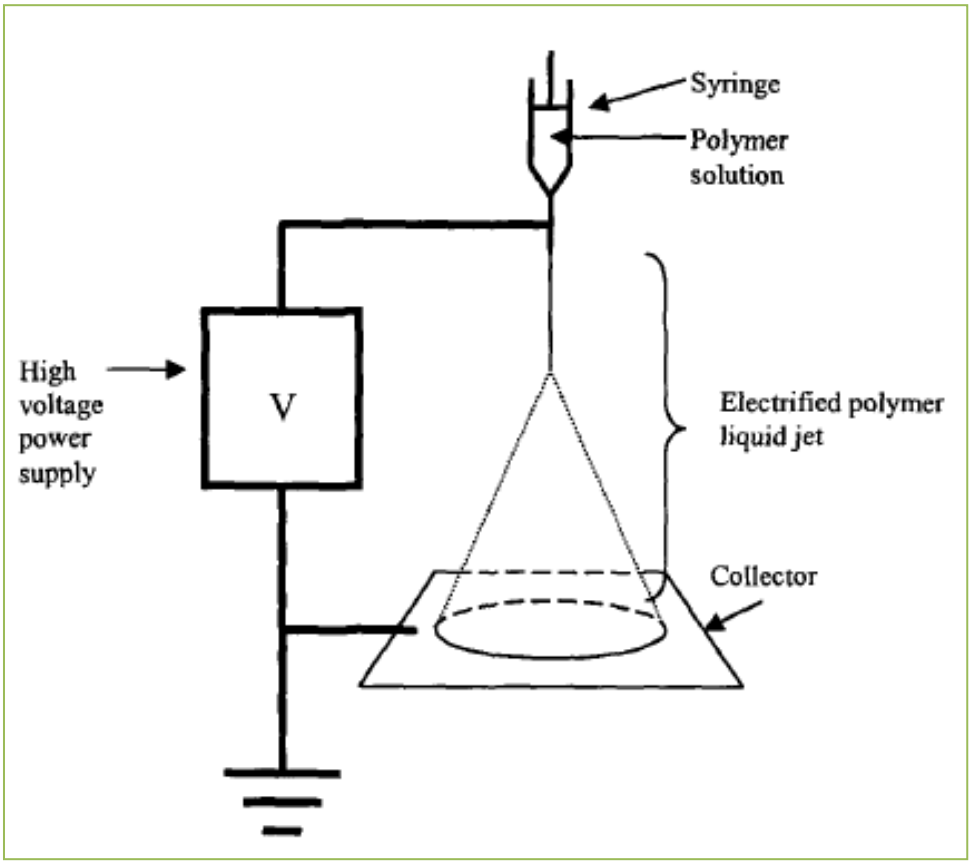

Figure 2. Schematic diagram of electrospinning process and apparatus [9].

In most cases, a high positive DC voltage of several tens of kV is applied to the polymer solution and the collector is grounded. A syringe pump is mostly used to flow the polymer solution out of the syringe at a constant flow rate. When the electric field is applied to the polymer solution in the syringe, charge is induced at the tip of the needle where the liquid is held together by its surface tension. Mutual charge repulsion causes a force directly opposite to the surface tension of the liquid. With the increase of intensity of electrical field, the shape of the liquid at the tip of the needle changes from a hemispherical shape to a more elongated conical shape known as Taylor cone [10]. Further increase of electrical field intensity takes the repulsive

force to a critical threshold level where it exceeds the surface tension of the liquid and a jet ejects from the tip of the Taylor cone. Charge repulsion inside the jet and the interaction between external electrical field and the jet causes it to experience a bending instability. The unstable jet starts to loop and stretch thinner with each loop until it reaches the collector. The solvent evaporates and leaves dry fiber on the collector. In cases where molten polymers are used for electrospinning, the jet solidifies as it travels through air. Hundreds of different polymers have been electrospun into nanofibers for various potential applications.

Features of the jet in electrical field are matter of great interest. There are experimental validations supporting the conical shape projection of liquid jet [10, 11]. With a semi vertical cone angle of 49.3°, it is possible to achieve fine jets of various liquids. A mathematical equation of critical voltage was developed by Taylor which is given below:

$$V_c^2 = 4 \times \left(\frac{H^2}{L^2}\right) \times \left\{\ln\left(\frac{2L}{R}\right) - 1.5\right\} \times (0.117 \times \pi \times R \times \gamma) \qquad (2.1)$$

where V_c is critical voltage, H is distance between tip and collector, L is length of capillary tube, R is radius of the tube and γ is surface tension of the liquid.

The surface tension mostly depends on the solvent composition and very little on the polymer [12]. The electric charge on the jet leads to bending instability due to repulsion and the fluid moves in an intricate path to lower the coulomb interaction energy. It was found that instability increases with increase of electric field strength and instability mostly relies on surface charge density and radius of the jet [13, 14].

2.2 Electrospinning Parameters

There are several parameters that influence electrospinning process and the resulting fiber morphology. These parameters can be grouped into three main types: (a) solution properties such as polymer molecular weight, solution viscosity, conductivity, surface tension and dielectric

constant of solvent; (b) process parameters such as voltage, distance between tip and collector, needle diameter and geometry, type of collector and flow rate; (c) ambient parameters such as humidity and temperature. Effects of these parameters are discussed in detail in this section

2.2.1 Solution Parameters

Solution parameters have profound effect on the resulting morphology of the electrospun fibers. Different polymers and solvents have different material properties. Therefore, proper understandings of the solution parameters are required to spin fibers of desired morphology.

2.2.1.1 Viscosity/Concentration/Molecular Weight of Polymer

Viscosity is one of the most influential factors in determining the fiber morphology. The viscosity of polymer solution increases with increase in the molecular weight of polymer and increase in concentration of the polymer in solution. To electrospin a fiber, the polymer must have an adequate molecular weight and similarly the polymer solution must have a sufficient level of viscosity. If the molecular weight is not enough, the jet tends to break apart on the way to the collector. The chain entanglement of very low molecular weight polymer or low concentration solution is not enough to prevent the jet from breaking up. Research results indicated that at very low concentration of polymer solution, fiber becomes non-uniform and beads tend to form on the fiber [15, 16, 17, 18]. The fiber diameter distribution is also likely to have a much larger spread as secondary jets might eject from the primary electrospinning jet. With the increase of polymer concentration, fibers become more uniform in morphology and free from beads [17, 18]. If the viscosity is too high, polymer solution might dry at the tip and produce no fiber at all [17]. Diameter of electrospun fibers tend to increase with increase in viscosity/concentration of solution [18]. Higher chain entanglement of polymer in high viscosity solutions resists the fiber from stretching and producing thin fiber. The specific surface area of

nanofiber decreases with the increase of fiber diameter which in turn reduces the surface functionality of nanofiber. Fibers are collected in a much smaller area on the collector in case of a highly concentrated polymer solution [9]. High viscosity of the solution probably resists the bending instability causing the fiber to be deposited in a much smaller area.

2.2.1.2 Surface Tension

The initiation of jet in electrospinning requires the repulsion to exceed the surface tension. Although the actual effect of surface tension on fiber morphology is not clear, it is assumed that surface tension causes the polymer chains to congregate and form beads in low concentration solutions.

2.2.1.3 Solution Conductivity

High conductivity of solution in electrospinning yields more uniform fibers with less beads and defects [15, 17]. The diameter of fiber also comes down with increase in conductivity [17]. In some cases researchers have added salt to the polymer solution to increase its conductivity in an effort to produce smaller diameter fiber with fewer amounts of defects [17, 19]. Results have shown that salt with smaller ionic radius produced smaller diameter fibers and vice versa [17]. It was assumed that higher charge density achieved from smaller ionic radius resulted in higher stretching force which reduced the diameter of fibers.

2.2.1.4 Dielectric Constant of Solvent

Dielectric constant of solvent also seems to affect the resulting morphology of electrospun nanofibers. Usually a solvent with high dielectric constant yields fiber with less bead formation and smaller diameter [20]. The deposition area on collector also increases due to higher bending instability. Although higher conductivity or dielectric constants generally yield smaller diameter fibers, compatibility of polymer with solvent has to be kept in mind. A polymer

is not chemically compatible with all types of solvents and therefore a compatible solvent must be chosen for electrospinning high quality nanofibers.

2.2.2 Process parameters

Process parameters are those variables which can be directly controlled during the electrospinning process. Process parameters also play vital role in determining fiber morphology.

2.2.2.1 Voltage

Applied voltage is a very important factor in the resulting fiber morphology and a much studied parameter. Sufficient voltage is required to exceed the surface tension of the liquid and initiate jet ejection. At low voltages, a nice Taylor cone is formed at the tip of pipette or needle and uniform bead free fibers are produced [18]. As the voltage increases, the cone formed at the tip tends to recede and thinner diameter fiber is produced, and bead formation tends to increase [18]. High voltage generally increases the bending instability causing jet thinning. At very high level of voltages, Taylor cone is often not visible at all as it retreats completely inside the needle [17, 18]. Some studies show interesting contradictory results suggesting the increase in fiber diameter with increase in voltage [21, 22]. It was suggested that high amount of bead probably aggregated to form thick fiber. It is also possible that accelerated speed of jet due to high electric field might reduce fiber stretching because the jet has less flight time at high speed. The ambiguous results suggest that applied voltage requires optimization for producing fibers of good morphology.

2.2.2.2 Distance between Tip and Collector

Distance between the pipette or needle tip and collector affects the electrospinning process and fiber morphology. Increasing the tip and collector distance increases the flight path of the jet which causes more elongation and yields thinner fiber. The increased flight time also

gives more time for the solvent to evaporate. If the distance between tip and collector is too small, wet fiber may deposit on the collector and merge together to create more interconnected pattern. This interconnected pattern might be useful for certain application such as scaffolds or sensors. Too high distance between tip and collector may increase bead formation and produces non-uniform fiber architecture.

2.2.2.3 Needle Diameter

The diameter of the pipette tip or needle also has an effect on the fiber morphology. Smaller internal diameter of needle decreases the droplet size at tip and consequently yields fiber of smaller diameter. Smaller diameter needle also prevents the solution drying up and the clogging as less solution is exposed to the environment. Reduction in tip diameter also reduces bead formation [23]. Tip should not be too small so as to prevent solution from flowing out. Solution containing nano-inclusions may clog at the needle if the diameter is too low.

2.2.2.4 Type of Collector

In most cases, the collector is a static metallic or non-metallic plate where the electrospun fibers deposit. When collector is made of conductive material, a high packing density of fiber is usually observed on the collector. However, in case of non-conducting collectors, the charge on the fiber cannot dissipate quickly as in a conductive collector. Therefore, the fibers repeal each other yielding a much porous structure and less packing density [24]. Porosity of collector also seems to have an effect on the resulting morphology. Fiber with less packing density is achieved in porous collectors [24]. Aligned fiber can be spun by using a rotating drum type collector instead of a static collector. Rotating collectors also help in the fast evaporation of solvents.

2.2.2.5 Flow Rate

Low flow rate usually yields fiber with smaller diameter [17]. When flow rate is increased, there is more solution available at the tip which increases the fiber diameter. The higher amount of solvent present while spinning at high flow rate may not have enough time to evaporate during the flight towards collector. The residual solvents may cause creation of further interconnects which can change the morphology of the fiber mat.

2.2.3 Ambient Parameters

Ambient conditions, such as humidity and temperature also affect the fiber morphology. At highly humid condition, small pores are created on the surface of the fiber and the amount of pores increased with increase in humidity [25]. Fiber diameter also tends to decrease with the increase in ambient temperature which is attributed to the reduced viscosity of polymer solution at higher temperature [16].

2.3 Fiber Morphology Optimization

The resulting morphology of electrospun fiber is affected by all the parameters discussed in section 2.2 and the effect of an isolated parameter is very difficult to predict due to the interaction of several different parameters. In most cases, a trial and error type approach is used to optimize the fiber morphology until the desired architecture is achieved [26].

2.4 Biosensors

A biosensor is a transducer that responds to biological or chemical stimuli and produces a functionally related response. Sensors are not just mere detectors. Sensors detect and quantitatively measure the measurand whereas detectors only specify the presence of a measurand. Biosensor is powerful modern day tool with application in healthcare, environmental

monitoring and defense application. This section discusses the fundamental concept of biosensors.

2.4.1 Working Principle

Development of POCT device has been a field of tremendous interest among the scientific community in recent years. Any biosensor should possess the desirable characteristics of an ideal sensor, such as continuous operation without affecting the measurand, fast response, high sensitivity, appropriate selectivity, high signal to noise ratio, reliable behavior and compactness. A biosensor combines a biological sensing element and a transducer to produce a measurable signal which is functionally related to the analyte concentration. The major components of a biosensor consist of: (a) a bio-receptor/analyte complex, (b) a molecular sensing and transduction element that converts the interaction of biomolecules into measurable signal and (c) a quantification and signal processing system. Figure 3 illustrates the major components of a biosensor.

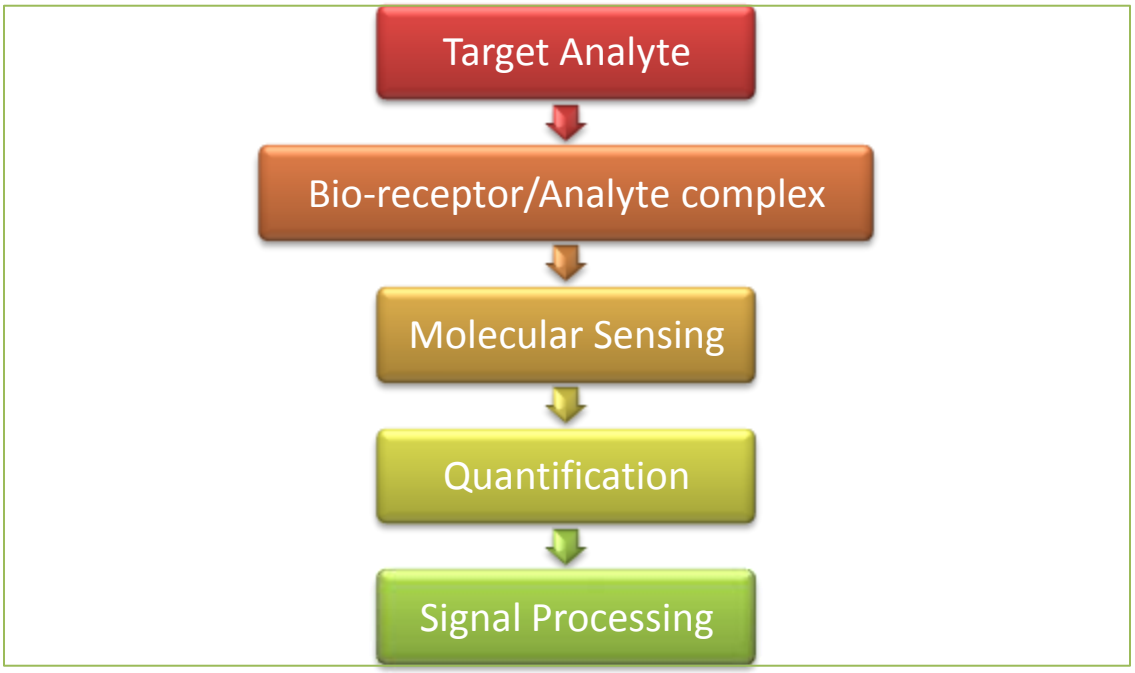

Figure 3. Process flow diagram of working principle of a biosensor

The bio-receptor is usually immobilized onto the sensing material or nanostructure with appropriate chemical functionalization which binds to the target biomolecule. Immobilization of receptors can be performed through adsorption or encapsulation or chemical functionalization. The bio-receptor/analyte complex can be any type of biomolecular interaction, such as antibody-antigen interactions, nucleic acid interactions, enzymatic interactions, cellular interactions or analyte/synthetic receptor interactions. The biomolecular interaction is sensed through various types of transduction platforms to produce a measurable signal which allows the quantitative measurement of the target biomolecule.

2.4.2 Label or Label Free?

Label free biosensors are those which do not use any reporter molecule, such as fluorescent, luminescent or calorimetric tag to provide the quantitative measure of the target analyte concentration. Most commercially available immunoassay uses some sort of reporter molecule and therefore requires dedicated laboratory facility and bulky equipments for analysis. The multi-step processes of attaching reporter molecules also make the assay time consuming. Development of label free biosensors enables the usage of unmodified samples, with possibility of sensitive real time assay. Smart label free biosensors can integrate several laboratory functions onto a single portable device and ensure fast diagnostics with the use of ultra-low sample volume.

2.4.3 Biosensor Characteristics and Terminology

Overall performance of a biosensor is determined by several performance parameters. This section discusses sensor characteristic parameters which are taken into consideration while monitoring the device performance.

2.4.3.1 Sensitivity

Sensitivity is the relationship between the sensor output signal and the measurand. Mathematically, it is the ratio of the incremental change in output to the incremental change of the input. High sensitivity of biosensor enables the detection of any biomolecule at very low concentrations.

2.4.3.2 Selectivity

Selectivity is the ability of a sensor to selectively detect the target in the presence of other molecules which may be present in the analyte. Selectivity is a very important parameter in case of immunosensors and also one of the biggest challenges in label free biosensor technology. Usually various non-target molecules are present at much higher concentration compared to the target biomolecule in the sample and therefore any cross-reactivity with the receptor or non-specific adsorption on sensing element may produce completely misleading results. In an effort to reduce non-specific binding, use of blocking agent has been a very common trend in label free immunosensors.

2.4.3.3 Limit of Detection

Limit of detection (LOD) is the lowest concentration of measurand that can be measured by the sensor. LOD is a very important performance measure of a biosensor. Immunosesnors with low LOD can help in early detection of disease biomarkers.

2.4.3.4 Dynamic Range

Range of a sensor refers to the range of (minimum and maximum stimulus) input signal that results in a meaningful output for the sensor. Outside the specified range, results obtained by sensors are unreliable.

2.4.3.5 Noise

Noise is the random fluctuations in the signal while the measurements are done. Noise can occur from both internal and external source. Noise reduction is very important while designing the device. High amount of fluctuation in output data may be difficult to interpret and may produce misleading results.

2.4.3.6 Drift

Drift refers to the change of output signal with time while the analyte concentration remains constant. Drift may arise from sensing material degradation, repeated usage and contamination. Long term stability of sensor components should be kept in mind while designing a sensor.

2.4.3.7 Hysteresis

Hysteresis is the difference in the output value at a certain level of measurand, when the measurand is approached first with an increasing and later with a decreasing stimulus.

2.4.3.8 Warm-up Time

It is the time required after the application of excitation energy before the senor starts to respond fully according to its rated specifications.

2.4.3.9 Response Time

It is the time required by a sensor to respond to a change in the input stimulus.

2.5 Antibody-Antigen Interaction

Antibody is a large Y-shaped protein which is used by the immune systems to detect and defuse unwanted foreign objects. The organisms that invoke immune response by antibody are known as antigens. Antibody identifies specific part of an antigen and therefore capable of

binding only to specific types of antigens. The antigen-antibody interactions are mediated by van der walls bond, hydrogen bond, ionic bond and hydrophobic interactions. The antibody and antigens have a mechanism similar to lock and key where only specific interactions are possible. Figure 4 illustrates the antigen-antibody interaction.

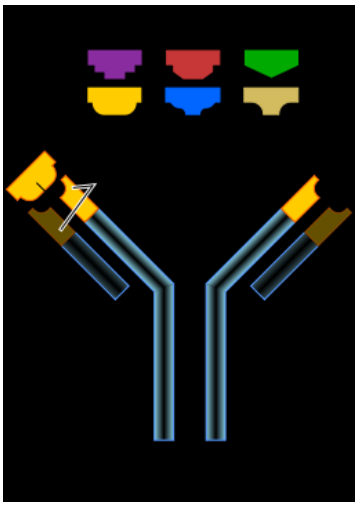

Figure 4. Specific interaction of antibody and antigen where the antibody only binds to the yellow color antigen.

As shown in Figure 4, the structure of the tip of the antibody only matches to the structure of a specific type of antigen and will only interact with that specific antigen. This interaction mechanism is the fundamental aspect of many label free biosensor where the binding and formation of this complex is sensed by a transduction platform to quantify the concentration of the measurand.

2.6 Nanotechnology and Biosensors

Use of nanomaterials and nanostructures revolutionized label free biosensor technology. Materials which are smaller than the characteristic dimensions exhibit fascinating size dependent chemistry and physics. High aspect ratio of nanomaterials increase the surface functionality and surface phenomena starts to dominate over the chemistry and physics in the bulk. Nanotechnology enabled sensors are build to take the advantages of these phenomena. With the

use of nanomaterials, sensitivity of sensors increases by a large margin since they are very sensitive to surrounding environment. Size matched confinement in nanostructures makes them ideal candidate for highly sensitive biomolecule detection. Better physical and chemical properties lead to rapid transduction of signal which enables real-time detection. Reduction in size of sensing and transduction element allows miniaturization of device onto lab-on-chip platforms. Direct detection becomes possible without the use of labels and very small quantity of sample can be analyzed to produce results. Nanostructures such as carbon nanotube, inorganic nanowire, metallic nanoparticles, quantum dots, nanoporous alumina membrane, diatoms, polymeric membranes and electrospun nanofibers can be used as sensing element for biosensors.

2.7 Transduction Platforms

Various transduction mechanisms can be coupled with sensing element to produce measurable signal that can be directly related to the concentration of the target analyte. Major transduction mechanisms are optical, electrical/electrochemical and mechanical transduction. Figure 5 shows the major transduction platforms and target analytes that can be bound to the bio-receptor.

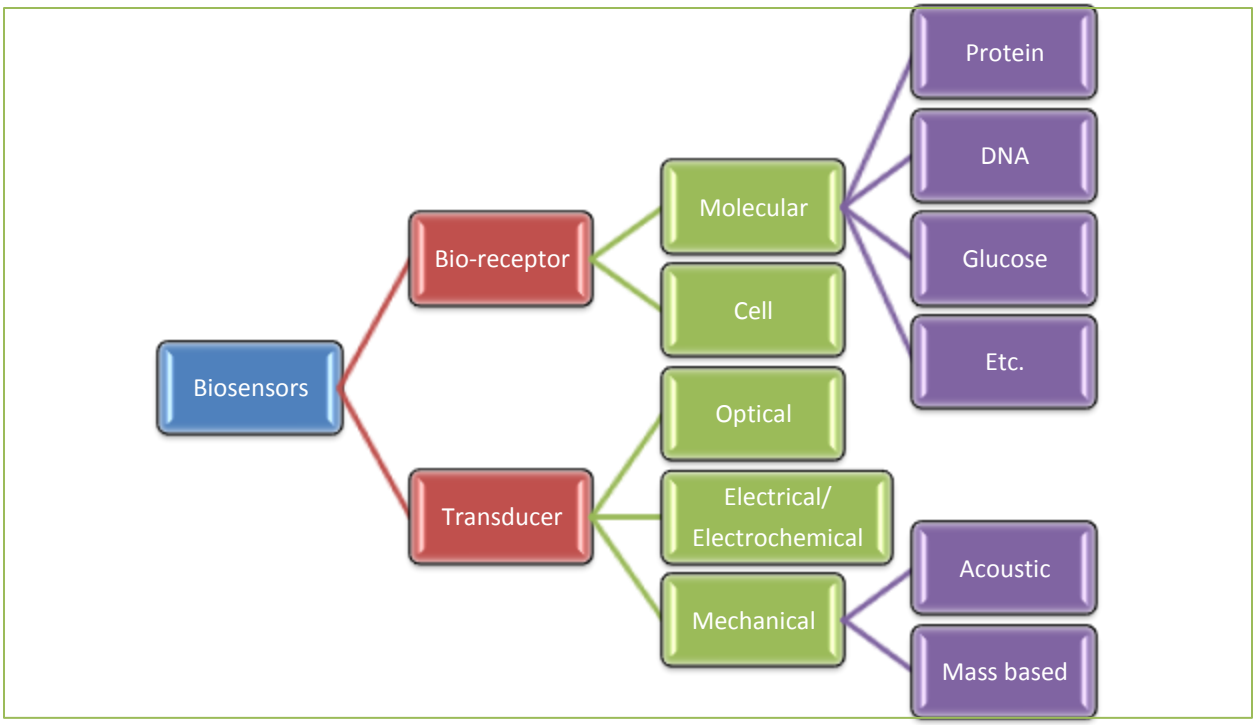

Figure 5. Types of biosensors based on transduction mechanism and target biomolecules.

2.7.1 Optical Detection

Optical detection techniques are widely used in current commercial immunoassays. Optical detection schemes are based on fluorescence, luminescence or light absorption. Usually a tag or reporter molecule is attached to the target which is activated when binding takes places. The intensity or color of light gives a measure of the target analyte. Nanomaterials such as quantum dots and gold nanoparticles are becoming popular as tags in recent times. Some popular label free optical detection methods are fiber optic biosensor, surface plasmon resonance biosensor (SPR), localized surface plasmon resonance biosensor (LSPR), surface enhanced raman scattering based biosensor (SERS), etc. Most of these techniques work on similar principal. Binding of target biomolecule and receptors on the sensing element modulates the intensity or wavelength or absorption.

SPR sensor is a very popular detection mechanism where the biomolecule binding event modulates the refractive index at the sensing layer which is mostly made out of gold (thickness in the order of nm). A light source is used to excite the surface plasmon (transverse electromagnetic wave on the thin metallic layer) which is very sensitive to the refractive index of the metallic sensing element and analyte interface. Biomolecular binding event (and therefore change in refractive index) shifts the surface plasmon resonance angle which can be probed through the shift in resonance angle or wavelength or intensity of the reflected light. LSPR uses a similar concept where surface plasmon in enhanced by using metallic nanoparticles. Nanoparticles show strong light scattering effect and enhancement in electromagnetic field. Although the label free optical detection techniques can be tailored to detect any analyte by appropriately preparing the sensor platform, proper sensing element functionalization is required to ensure selective binding of target molecules. These techniques are also susceptible to background interference and ambient parameter fluctuation.

2.7.2 Electrical/Electrochemical Detection

Electrical and electrochemical detection principles gained huge popularity in biosensor technology due to the ease of these techniques and better control over electrical properties of materials in small scale. Major class of electrochemical detection techniques are potentiometric, amperometric and conductimetric/impedimetric biosensors.

Potentiometric sensors measure the oxidation and reduction potential of an electrochemical reaction. When a ramp voltage is applied to the electrochemical systems, a current flow occurs due the reaction that takes place. Voltage at which these reactions take place and the magnitude gives a quantitative measure of a particular species.

Amperometric detection techniques probe the movement of electrons produced by a redox reaction in the electrochemical system. In case of non-electroactive biomolecules, redox mediators are used to catalyze the production of redox species.

Another type of detection technique is called conductimetric/impedimetric detection. The conductivity or resistivity of the analyte changes when an electrochemical reaction creates ions or electrons. The conductance or resistance change is measured to quantitatively determine the concentration of the measurand.

Field effect transistor (FET) based detection is a popular category of electrical biosensor. Nanomaterial such as carbon nanotube or inorganic nanowire is used as the channel of the FET and functionalized with appropriate bio-receptor. Binding of target biomolecule modulates the gate voltage of the FET which causes a shift in drain current. The change in drain current can be correlated to the concentration of the measurand.

2.7.3 Mechanical Detection

Mechanical detection based biosensors are mainly mass sensitive in nature. Quartz crystal microbalance (QCM), surface acoustic wave (SAW) and micro-cantilever based biosensors are some popular mechanical detection scheme based biosensors.

In QCM biosensors, the change in resonant frequency of a quartz crystal due to biomolecule binding is probed to get a quantitative measure of the target biomolecule. SAW biosensor makes the use of a surface propagating acoustic wave on the transducer platform. Application of AC voltage in the input interdigital transducer creates an acoustic wave that propagates through the sensing area towards the output interdigital electrodes. The acoustic wave is highly sensitive to mass loading on the propagation pathway and therefore any biomolecule binding on the transducer can be probed by monitoring the change in the velocity and phase

angle shift of the propagating wave. Microcantilevers respond to mass loading by changing the vibrational frequency or deflection. This principle can be used to sense biomolecules if the microcantilever is functionalized with the appropriate bio-recognition element.

2.8 Sensor Applications of Electrospun Nanofibers

High specific surface area and porosity makes nanofiber an ideal candidate for sensor applications. To date, electrospun nanofibers have been mostly used for gas sensing. Lithium perchlorate ($LiClO_4$) doped polyethylene oxide (PEO) nanofiber was used as the sensing element of an electrochemical sensor for humidity sensing [27]. Camphorsulfonic acid (HCSA) doped polyaniline (PANI)/polystyrene (PS) electrospun nanofiber was used to detect hydrogen peroxide and glucose [27]. An electrospun PANI/PEO based field effect transistor biosensor was reported by Pinto et al. [28]. Urease incorporated electrospun polyvinylpyrrolidone (PVP) nanofiber was fabricated for urea sensing which can detect liver and kidney malfunction [29]. PANI/PVP composite nanofiber was successfully used to detect presence of NO_2 [30]. Electrospun tungsten oxide (WO_3)/Polyvinyl acetate (PVAc) nanofiber was used for detection of ammonia [31]. A QCM biosensor was reported with electrospun polyacrylic acid nanofiber as the sensing element for ammonia detection [32]. Fluorescent probe was self assembled electrostatically on electrospun cellulose acetate (CA) to fabricate an optical biosensor for methyl viologen and cytochrome detection in aqueous solution. Recently, use of electrospun polystyrene (PS)/polypyrrole (PPy) nanofiber for electrochemical detection of cardiovascular disease biomarker was reported by Kunduru et al. [33]. Results indicated the enormous potential of electrospun nanofiber for protein detection.

2.9 Recent Biosensor Developments: Application to CRP Detection

Several optical, electrical/electrochemical and mechanical transduction mechanism based biosensors have been reported in recent years for CRP detection. This section discusses about some of the interesting findings of the research community on CRP detection.

2.9.1 Optical Sensors

A microchip-protein assay containing an array of microcavities etched in a silicon wafer was developed [34]. Agarose beads were made to fill the microcavities and each of twelve wells served as a microanalysis chamber. As the analytes passed around the beads, antigen-antibody reaction was enhanced due to mixing. In the discussed research work, the analyte was CRP conjugated with Alexa 488 fluorophore. The fluorescence on the beads upon binding was observed using CCD camera and digitally processed. A modified surface plasmon resonance biosensor based on gold and silicon dioxide nanoparticle embedded in the dielectric film was reported [35]. The metal surface was composed of mixed gold and silicon dioxide nanoparticles and the layer was made by co-sputtering. Bhattacharyya et al. developed a microfluidic immunosensor and CRP was detected using chemiluminescence [36]. Luminol was used as substrate and HRP enzyme as secondary antibody. HRP oxidized luminol and when the latter returned to its original state, iridescent blue light was emitted. This was detected using instant film or imager capable of measuring chemiluminescent signal. Surface Plasmon resonance based biosensor was developed with aptamer immobilized on the gold layer [37]. This aptamer specifically interacts with CRP leading to a shift in resonance. Kim et al. reported detection of CRP using localized surface plasmon resonance (LSPR) [38]. A porous anodic alumina (PAA) layer was fabricated consisting of inter-pores. Gold was made to form a ‘cap’ on the PAA layer. This formed the sensing element on which anti-CRP was immobilized. The major advantage of

this work is that with gold capped PAA layer, it is possible to measure change in refractive index and wavelength shift during one event using an optical fiber. Kim et al. reported a self assembled monolayer using poly(thiophene) polymer on gold coated quartz cell [39]. This formed the sensing element on which anti-CRP was immobilized. Binding was detected using surface plasmon resonance (SPR). The reason for using poly(thiophene) was that it could react with amine bearing molecules at side groups and this reaction could be detected. Padigi et al. detected CRP biomolecule using cylindrical optical micro-waveguide based biosensor [40]. Binding of molecules on the waveguide surface altered the light intensity and its path. These variations could be used for detection. Cylindrical geometry provided the advantage of multiple reflections of photons at a given point. High aspect ratio triangular nanoplate (TSNP) was used as sensing element for CRP detection [41]. TSNP was functionalized with phosphocholine which acted as the receptor for CRP. LSPR was employed to detect the binding event. The sensitivity was increased a lot when TSNP was used with LSPR. An automated new microfluidic system has been developed for CRP detection [42]. A new CRP-specific DNA aptamer was conjugated to magnetic beads. CRP was added to the mixing chamber of the microfluidic system and incubated with the modified magnetic beads. Then anti-CRP labeled with Acridinium ester was then added to give chemiluminescence which was detected using photomultiplier tube.

2.9.2 Electrical/Electrochemical Sensors

Gul et al. reported two approach of detecting CRP; one method is based on microelectrode and the other on microarrays [43]. For the microelectrode based detection, an interdigitated capacitive electrode was used. Binding modulated the dielectric constant between the electrodes which was measured using an AFM and electrochemical methods. For the microarray based detection, a modified glass substrate was used. A fluorescent-tagged sandwich

structured antibodies were detected using optical scanner system. An interdigitated gold electrode on nanocrystalline diamond surface was reported as the sensing element for a capacitive biosensor [44, 45]. Antigen-antibody interaction was measured in terms of change in capacitance/ dielectric constant. The nanocrystalline diamond surface formed the dielectric layer between gold electrodes.

Kunduru et al. developed a biosensor based on platform-based microelectrode array (MEA) [46]. Antibody functionalized polystyrene beads were used to from a microbridge between microelectrodes by means of electrophoresis. A specific volume of CRP was added for binding to take place on the beads. The electrical signal from the binding interaction was enhanced due to coupling effects between beads. The amplified signal was measured using nanovoltmeter. Bothara et al. used a nanostructured alumina membrane to immobilize anti-CRP in nanowells [47]. Binding caused perturbation in electrical double layer leading to change in capacitance which was measured. Use of biogenic nanoporous silica as sensing element was reported [48]. Biogenic silica consists of nanowells which were used for biomolecule entrapment. Antibodies were immobilized on the gold surface at the bottom of nanowells and its binding with CRP led to the formation of electrical double layer. This would lead to change in the impedance which was measured by electrochemical impedance spectroscopy. Kunduru et al. used polypyrrole coated polystyrene nanofiber as the sensing element to detect CRP [33]. Nanofiber morphology provided the size match confinement for protein immobilization. The performance of electrospun nanofiber was compared with polystyrene microsphere mat. The nanofiber gave significant enhancement in signal compared to the beads proving the size match confinement theory. Results indicated that scaling down to nanoscale increases the sensitivity of biosensors.

Sohn et al. used Au/NiCr on the gate surface of FET biosensor [49]. Cysteine tagged protein G was made to form a layer on the gate surface which then facilitated the immobilization of anti-CRP. Binding of antigen-antibody of CRP was measured in terms of changes in the drain current.

3D nanogap gold interdigitated microelectrode was used to detect CRP and design optimization of electrode geometry was studied [50]. The authors investigated effects of electrode width, gap and height on electric field and current density in order to obtain an optimum geometry. Height and gap between electrodes play an important role in electric field and current. They observed microelctrodes possessing gap and height between 200 and 500 nm provided improved electric field and current density distribution. To detect binding events electrochemical impedance spectroscopy was used. Silicon nanowire array was used as the sensing element in FET biosensor [51]. A top down approach based on photolithography, anisotropic etching and thermal oxidation was used to fabricate the sensor.

Aptamer which would specifically bind with CRP was immobilized on to gold interdigitated array electrodes of a capacitive biosensor [52, 53]. Binding between aptamer and CRP led to changes in dielectric parameters which were measured by non-Faradaic impedance spectroscopy (NFIS).

2.9.3 Mechanical Sensors

Piezoresisitive microcantilever with functionalized gold surface was used to detect CRP [54]. Antigen-antibody binding led to changes in stress on the cantilever and hence caused bending of the cantilever. This would change the resistance of the peizoresistive layer which was measured. Chen et al. reported the use of micro electrochemical systems (MEMS) microcantilever to detect CRP [55]. The deflection resulting from antiCRP-CRP binding was

measured using a position-sensitive detector. Optical beam deflection was utilized for measurement of cantilever bending as this technique provided minimum detection limit of 0.1 nm. Chromium and gold were deposited on the cantilever to immobilize anti-CRP.

CRP has been detected using a technique called resonant acoustic profiling (RAP) [56]. In this method, a high frequency voltage was applied across a piezoelectric crystal and the resonant frequency was observed in real time. The instrument consisted of four channels allowing four simultaneous measurements. The sensing element consisted of quartz wafers with gold coating and carboxylic acid terminated coating for protein immobilization. CRP was detected in three different ways and the results were compared with conventional ELISA technique. For direct detection, sample of CRP in buffer was injected onto the sensing element functionalized with sheep anti-CRP. For homogeneous sandwich assay, sheep anti-CRP was added to CRP sample in buffer before injection and for direct sandwich assay, anti-CRP antibody was injected after the direct detection step. For control experiment, sensing element was functionalized with sheep immunoglobulin type G. The results using RAP was comparable to conventional ELISA technique. Yatsuda et al. developed a biosensor based on shear horizontal surface acoustic wave and detected human serum albumin and CRP with it [57]. The sensor device consisted of shear horizontal surface acoustic wave (SH-SAW) delay line fabricated on quartz. The sensing element possessed a gold film to which antibodies were immobilized by means of linker. The device contained an electric reader which measured the antigen-antibody interaction in terms of velocity or attenuation changes. Table 1 shows the detection principle and performance parameters of various biosensors designed for CRP detection.

TABLE 1

BIOSENSOR FORMATS APPLIED TO CRP DETECTION

Signal Transduction	**Assay Format and/or Nanostructures Used**	**LOD**	**Sample Vol. (µl)**	**Assay Time (hrs)**	**Ref.**
Fluorescence	Agarose microbeads	1ng/ml	-	1.25	34
SPR	Co-sputtered Au and SiO_2 nanoparticles	1µg/ml	-	>24	35
Chemiluminescence	Luminol substrate and HRP enzyme	1.85µg/ml	75nl	-	36
SPR	Aptamer	0.005ppm	20µl	-	37
LSPR	Gold capped porous alumina	1pg/ml	15µl	5	38
Fiber optic	Cylindrical micro cavity based waveguide	10pg/ml	-	<0.5	40
LSPR	High aspect ratio triangular silver nanoplate	5ng/ml	-	-	41
Chemiluminescence	Aptamer conjugated magnetic beads	12.5ng/ml	5µl	2.5	42
Capacitive	Gold interdigitated electrode on nanocrystalline diamond surface	25ng/ml	20µl	9	44, 45
Capacitive	Microelectrode and microarray	2.2ng/ml	2µl	3	43
Dielectrophoresis	Polystyrene microbeads	1µg/ml	-	-	46
Capacitance	Nanoporous alimuna	200pg/ml	-	-	47
Impedance	Biogenic nanoporous silica	1pg/ml	10µl	0.75	48
Impedance	Electrospun PS fiber coated with PPy	1pg/ml	200µl	3	33
FET	Au/NiCr as channel	3µg/ml	-	-	49
Impedance	3D nanogap gold interdigitated microelectrode	13ng/ml	-	12	50
FET	Silicon nanowire array	1 fM	-	<0.5	51
Capacitance	Aptamer	100pg/ml	-	12	52, 53
Mass loading	Piezoresistive microcantilever with functionalized gold surface	100ng/ml	-	4	54
Mass loading	Microcantilever with gold surface	1µg/ml	-	1.25	55
Acoustic	Gold coated quartz wafer	3ng/ml	-	<0.5	56
SH-SAW	Gold coated quartz substrate	50ng/ml	-	<0.5	57

CHAPTER 3

MATERIALS AND METHODS

3.1 Electrospinning Polymer Blend Fibers

A blend of Polystyrene and Polyaniline was used for electrospinning nanofibers which were used as the transduction platform for the biosensor. Subsequent sections discuss in detail about the polymers used and the process used for nanofiber fabrication.

3.1.1 Polystyrene

Polystyrene (PS) is a polymer made from the monomer styrene. It is one of the most widely used polymers. Polystyrene is an odorless, tasteless, rigid thermoplastic, which is in solid state at room temperature, but becomes liquid if heated above the glass transition temperature (~95°C). It is a long chain hydrocarbon where alternating carbon centers are attached to phenyl groups. Chemical structure of monomer styrene and polystyrene is shown in Figure 6.

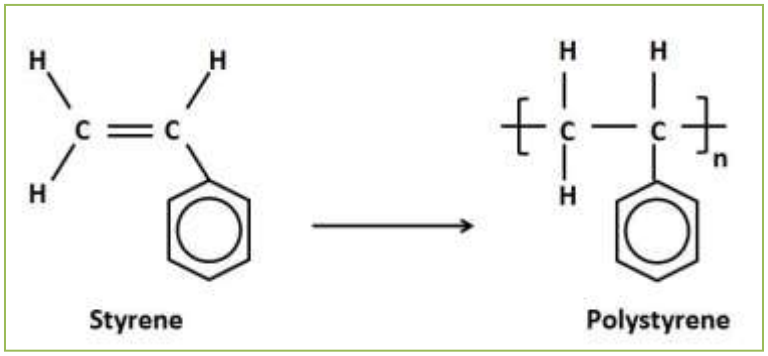

Figure 6. Chemical structure of styrene monomer and polystyrene.

Polystyrene is the most commonly used material in a solid-phase immunoassay. It offers a biocompatible hydrophobic surface. Polystyrene was used in conjunction with polyaniline for its ease of electrospinning and processing. Polystyrene acts as a solid phase support that helps protein immobilization through passive hydrophobic adsorption. The adsorption mainly takes place through van der waals attraction between the hydrophobic areas of the absorbed ligand and

polystyrene surface. However polystyrene itself is not conductive enough to act as the transduction platform for a biosensor. Polystyrene was purchased from Sigma Aldrich (Product Code# 430102, MW 230000, T_g 94°C).

3.1.2 Polyaniline

Polyaniline is a unique member in the family of conductive polymers. Its distinctive feature is that it can act as a semi-conductor. It can be manipulated to act as purely non-conductive polymer and also as highly conductive polymer for various electrical applications. When it was discovered in 1934 and it was used to be known as 'aniline black'. Polyaniline's flexibility and its use became apparent in late 1990. One of the major problems with conducting polymer was that there was no known example of stable metallic polymer even in the early 1990. Polyaniline has solved this problem and it offers several other important advantages in terms of processing: monomer styrene is inexpensive; polymerization is relatively easy and it has high stability. It could be used for various applications such as intelligent windows, computer chips etc. One of the most desirable properties of polyaniline is its easiness in combining with other polymers to form the required shape. This was one of the reasons why it became so popular in various applications. It is very popular in computer industry where it is used in static free packaging, flexible electronic components and also as shield against electromagnetic radiation. Researches involving new applications of this polymer are underway. Manufacturers and researchers are taking advantage of the versatility of this material to find wide range of applications. Potential field of present and future application of polyaniline is in antistatics, actuators, electromagnetic interference shielding, supercapacitors, fuel cells, smart windows, heavy metal recovery, solar cell applications etc.

Polyaniline is doped by exposing it to other chemicals according to its required level of conductivity. Doped polyaniline is able to conduct electric current consistently and it also forms a more stable polymer. Doping of polyaniline involves partial oxidation or reduction which leads its conductivity. It is possible to obtain the desired level of conductivity for a particular application with polyaniline compounds. With various polyaniline blends it is possible to achieve high conductivity like in silicon and germanium and also highly insulating behavior as in glass. Polyaniline can be processed while it is molten form and also when it is in solution. This gives polyaniline the advantage of being blended with conventional polymers and that it can be easily formed into the desired shape. Disposal of polyaniline compounds are environmentally friendly. The electrical conductivity of polyaniline based compounds can be varied over a wide range. Figure 7 exhibits the chemical structure of polyaniline.

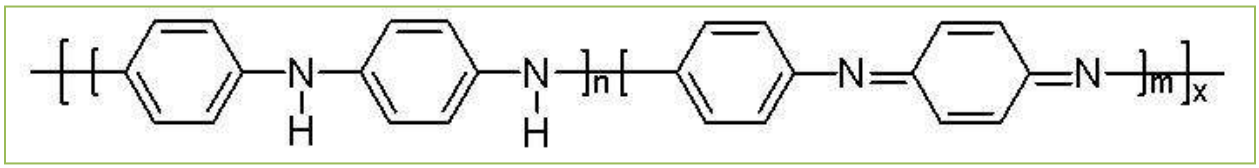

Figure 7. Chemical structure of polyaniline (n+m=1 and x=degree of polymerization).

The five different oxidation states in which polyaniline can exist are as follows:

1. Emeraldine (neutral or only partially reduced/oxidized), n = m = 0.5
2. Protoemeralsine, n = 0.7, m = 0.3
3. Leucoemeraldine (fully reduced state), n=1, m=0
4. Nigraniline, n = 0.3, m = 0.7
5. Pernigraniline (fully oxidized state containing imine links), n = 0, m = 1

Polyaniline used for experiments were purchased from Sigma Aldrich (Product code# 530689, MW 65000). Although polyaniline has huge potential to be used in biosensor, it is

difficult to electrospin. That is why polyaniline was blended with polystyrene to create the blend fiber mat.

3.1.3 Doping Polyaniline

Emeraldine base polyaniline (n=m=0.5) can be neutral or only partially reduced or oxidized. Emeraldine base polyaniline shows great stability relative to Leucoemeraldine which is easily oxidizable or to Pernigraniline which is easily degradable. That is why emeraldine base polyaniline is so popular.

In case of emeraldine base polyaniline, the electronic structure of constituent C_6 units leads to energy band gap. This distinguishes emeraldine base polyaniline from other types of conducting polymers such as polythiophene or polyacetylene where energy band gap arises from changes in bond lengths. It is possible to turn emeraldine base polyaniline from being an insulator to metallic like state by adding protons to the imine nitrogen of the base and keeping number of electrons in the chain constant. Sometimes protonation by an acid like nitric acid, hydrochloric acid or sulfuric acid can turn emeraldine base polyaniline to act as a semiconductor.

Emeraldine base polyaniline can also be protonated using organic acid such as camphorsulfonic acid (HCSA) or picric acid. A technique called solid state protonation can be used to protonate polyaniline using organic acid in their solid state and the conductivity achieved through dry solid state protonation is not significantly different from wet protonation that are done in presence of solvents. Emeraldine base is converted in the presence of camphorsulfonic acid into the protonated emeraldine form of polyaniline. Figure 8 shows HCSA and the chemical reaction during protonation.

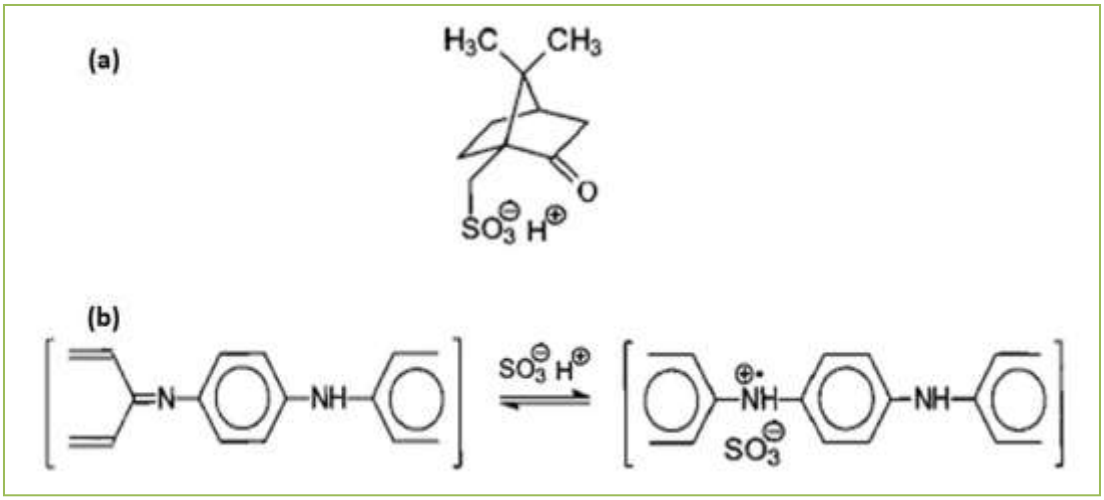

Figure 8. Doping of PANI; (a) Chemical structure of camphorsulfonic acid (HCSA); (b) Scheme of Protonation of polyaniline with HCSA.

HCSA donates its proton to the imine nitrogen of the emeraldine base. This positive charge on polyaniline is balanced by the anion of HCSA. The imine nitrogen donates an electron to the neighboring ring to convert it into benzoid. The remaining unpaired electrons on the nitrogen lead to electrical conductivity of protonated polyaniline although polyaniline base and HCSA are both non-conducting in nature.

HCSA was purchased from Sigma Aldrich (Product code# 147923). Polyaniline was mixed with HCSA in 1:2 weight ratio and ground thoroughly in a mortar-pestle for 30 minutes. The mixture was then heated at 85°C for 1 hour in an oven to increase its electrical conductivity.

3.1.4 Stock Solution Preparation and Electrospinning

A mixture of 2 wt% PANI, 4 wt% HCSA and 7.5 wt% PS was dissolved in chloroform to prepare the stock solution. After solid state Protonation of PANI-HCSA, PS and chloroform (Fisher Scientific, Product code# $C606^{SK}$-4) were added to the mixture. The solution was stirred magnetically overnight to produce a homogeneous solution. Figure 9 shows the stock solution of PS/PANI-HCSA.

Figure 9. Stock solution of PS/PANI-HCSA which was used for electrospinning.

A syringe pump was used for electrospinning. Figure 10 shows the setup for electrospinning. The distance between the tip of the syringe and collector was 300 mm and the applied voltage was 25 kV DC. An aluminum foil was placed onto the grounded counter electrode. Three different flow rates (0.5, 1.0 and 2.0 ml/hr) were used to spin PS/PANI-HCSA nanofiber mats. All other parameters were kept constant. The fiber mat was peeled off from the aluminum foil for further use.

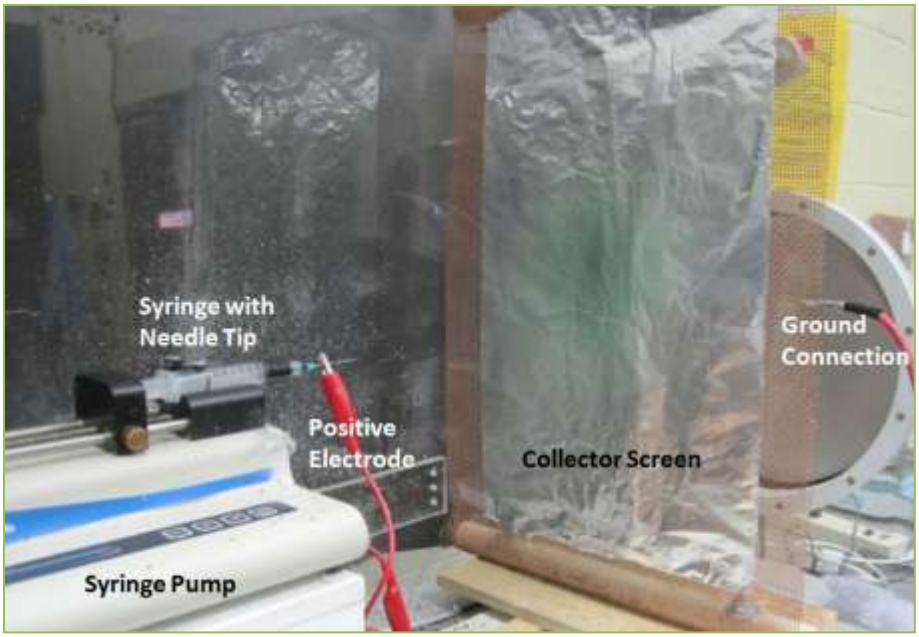

Figure 10. Digital image of the setup used for electrospinning.

3.2 Sensor Platform

The biosensor was based on a gold microelectrode platform. PS/PANI-HCSA nanofiber was placed on the gold microelectrode as the sensing element and a microfluidic encapsulation of 150 µl was created by attaching a manifold with inlet and outlet port on top of the chip.

3.2.1 Interdigitated Chip

The chip had an interdigitated pattern of gold electrode on top of it. Figure 11 shows a digital image of the interdigitated chip. The comb shaped pattern of the working and counter electrode ensures enhanced electrical field which improves the transduction performance of the device.

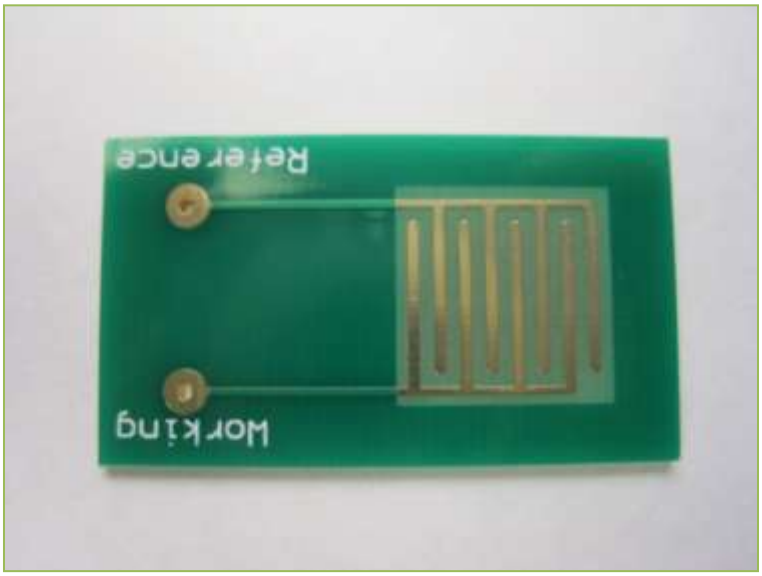

Figure 11. Digital image of interdigitated microelectrode chip.

3.2.2 Manifold Preparation

A manifold was made from polydimethylsiloxane (PDMS) to confine 150 µl liquid on the sensor surface. The manifold had two flow channels for inlet and drain of liquid. A master mold made of aluminum was used which could make 12 manifolds at a time. The master mold was

machined from an aluminum block using a HASS CNC machine. Figure 12 shows the image of the master mold and the prepared manifold.

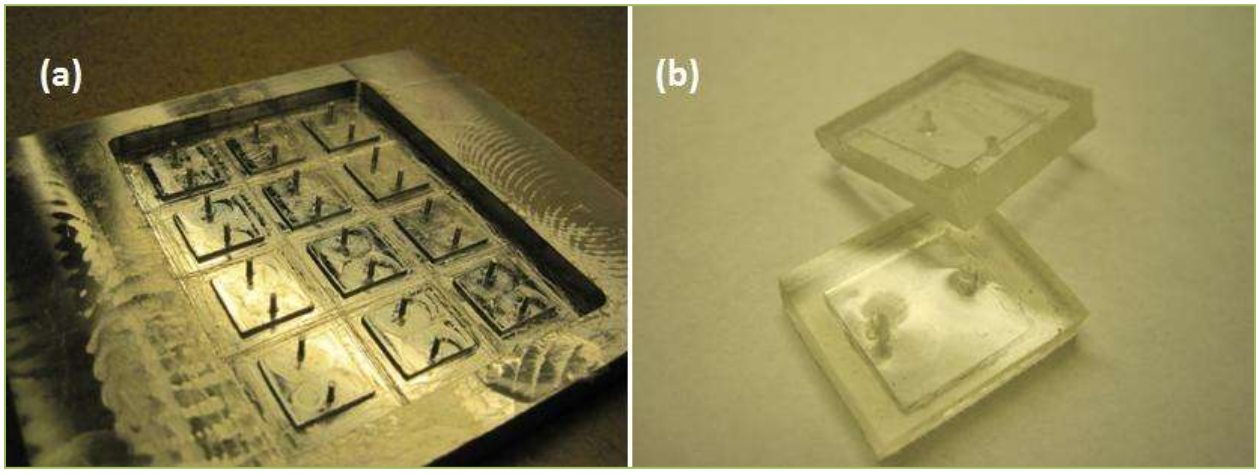

Figure 12. PDMS manifold for microfluidic encapsulation of analyte; (a) Master mold for making PDMS manifold, (b) PDMS manifold after peeling off from the mold.

The procedure for preparing PDMS manifold on the master mold is described below:

- The master mold was washed thoroughly with ethanol and air dried.
- First coat of mold release agent was applied onto the master mold using a hand sprayer and left for 15 minutes.
- Second coat of mold release agent was applied in similar fashion and left for 30 minutes so that the surface was properly dried. This mold release agent prevented the PDMS manifolds from sticking to the master mold.
- PDMS hardener and resin was mixed in 1:10 volume ratio and poured onto the master mold.
- The master mold was placed on a hot plate and the temperature was set to 100°C.
- PDMS was cured for 15 minutes on the hot plate and then the hot plate was turned off.
- Master mold was left to cool down to room temperature.
- A sharp laboratory knife was used to cut the 12 pieces of manifold and peel them off from the mold.

3.3 Chip Integration for Experiment

The interdigitated chip, electrospun PS/PANI-HCSA nanofiber mat and PDMS manifold were integrated together to create a smart and portable lab-on-chip platform for protein detection. Extension wires were soldered to the working and counter electrode terminals so that the biosensor can be hooked up to a potentiostat for electrical measurements. Figure 13 shows the assembled lab-on-chip device.

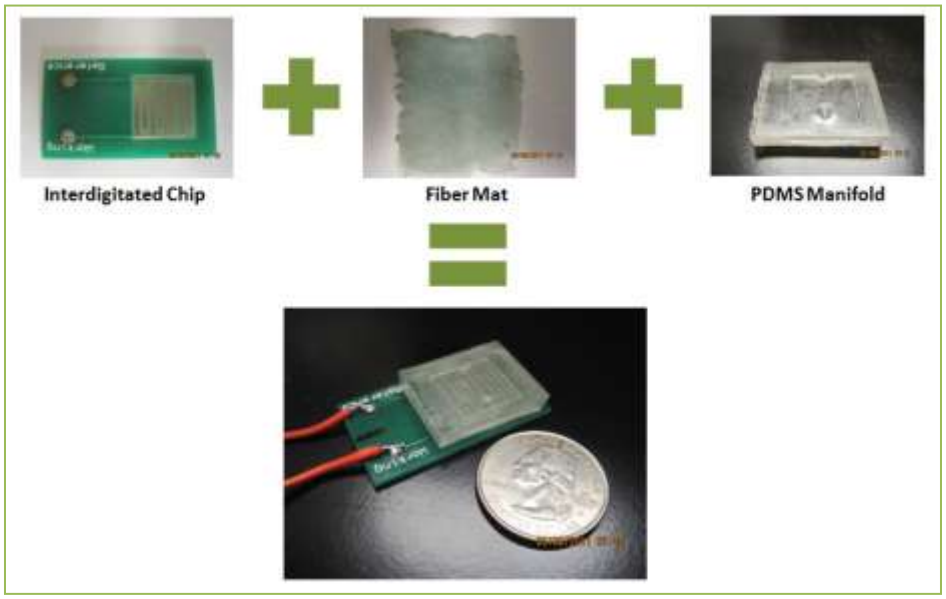

Figure 13. Assembled chip showing the different components and comparison of size with a quarter dollar coin.

3.4 Materials for Sensor Experiments

The study protein was human serum C-reactive protein (CRP) which is an inflammatory biomarker. CRP is indicative of cardiovascular disease and high level of CRP (>1.0 ng/ml) is considered as risk predictor for vulnerable coronary plaque rupture. The following sub-sections discuss about the study protein, its bio-receptor anti-CRP and other materials used for assay.

3.4.1 C Reactive Protein

C-reactive protein (CRP) was first discovered in human blood serum of patients suffering from acute inflammation in 1930 by Tillett and Francis. CRP belongs to ‘Pentraxins’ family of proteins [58]. It is known to be a plasma protein which takes part in the systemic response to inflammation. It is produced by liver. Molecular configurations that are result of cell death or presence of pathogens bind to specific sites of CRP molecules. Its concentration rises rapidly within hours after tissue damage and infection, revealing its contribution towards host defence [58]. Thus it can be used as early marker for infection, inflammation and tissue injury. CRP is made up of five identical non-covalently associated subunits called protomers which form symmetrical rings around central pore [58]. The diameter of protomer is 36 Å and that of the whole CRP pentamer is 102 Å. The inner core has a diameter of 30 Å. Figure 14 shows the crystal structure of C-reactive protein.

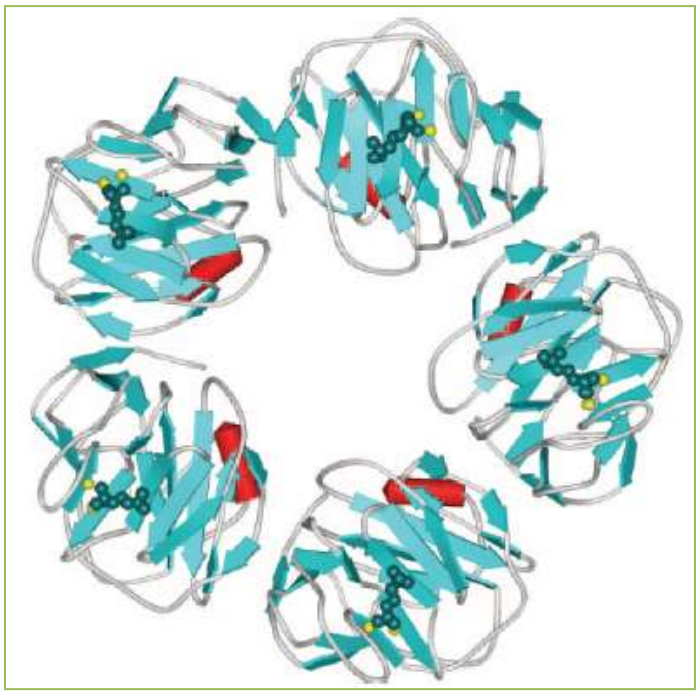

Figure 14. Crystalline structure of CRP complexed with phosphocoline [58].

X-ray crystallography studies have revealed that each protomer is folded into two anti-parallel β sheets with alpha helix on the effector face of the CRP protein. The protomer is made up of 206 amino acids. Each protomer possesses specific binding sites consisting of two coordinated calcium ions beside a hydrophobic pocket [58]. These form the binding sites for phosphocholine. The opposite face of the protomer forms the effector face on which binding of complement C1q and Fcγ receptors take place [58]. A cleft running from center of the protomer to the central pore possesses some residues on its boundaries and these play important role in binding of CRP to C1q, Asp-112 and Tyr-175 [59].

The biological function of CRP is mediated by binding with its ligands or its interaction with the effector molecules. Phosphocoline is present in various bacterial species. In normal cells, the head group of phosphocoline is not exposed to CRP. Thus CRP binding sites only becomes available to phosphocoline in damaged cells. CRP can also bind with various other types of ligands. Accumulation of CRP or its binding with ligands triggers classical complement pathway. CRP can interact with immunoglobin receptors, FcγRI and FcγRII to trigger phagocytic response. Therefore, CRP plays an important role in first line of host defense.

CRP is closely related to cardiovascular disease. CRP is a marker for peripheral arterial disease and sudden cardiac death [60]. CRP is a better biomarker than LDL cholesterol [60]. CRP levels of less than 1, 1 to 3 and greater than 3 ng/ml exhibit low, moderate and high risk of cardiovascular event respectively [60]. Arterial damage can be caused by white blood cell attack and inflammation with its wall. As CRP is a biomarker for inflammation, its level rises when there is arterial damage or blockage. Diabetes and hypertension can also cause high level of CRP [61]. CRP can also be used as a marker for stress. It is thus important to develop portable devices

sensitive enough to detect CRP at clinically relevant concentration. CRP was purchased from Abcam (Product code# ab51784)

3.4.2 Anti C-Reactive Protein

The antibody used in biosensor assay was Anti-CRP which selectively binds to only CRP. Anti-CRP was purchased from Abcam (Product code# ab10028).

3.4.3 DSP Linker

Dithiobis[succinimidyl propionate] also known as DSP linker is a thiol cleaveable, amine reactive crosslinker which possesses N-hydroxysuccinimide (NHS) ester reactive ends and a cleavable disulfide bond in the spacer arm. At each end of 8 carbon spacer arm of DSP, there is an amine reactive NHS-ester. NHS ester forms stable amide bonds releasing N-hydroxy-succinimide group by reaction with primary amines at pH 7-9. Figure 15 shows the chemical structure of DSP linker.

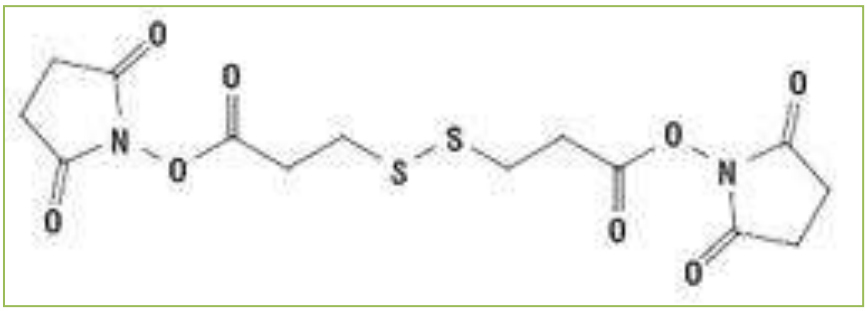

Figure 15. Chemical structure of DSP linker.

Antibodies possess several primary amines in the side chain of lysine (K) residues and the N-terminus of each polypeptide. These binding sites in proteins and antibodies are available to react with NHS-ester crosslinking reagents. DSP linker is used to chemically functionalize the PS/PANI-HSCA surface for anti-CRP immobilization. DSP was purchased from Pierce (Product code# 0022585).

3.4.4 BSA Block

Bovine serum albumin (BSA) superblock was used as the blocking solution for the assay which ensured selective binding of CRP only onto the complementary antibody and prevented non-specific adsorption of non-target molecule on the nanofiber surface. BSA block was purchased from Pierce (Product code# 0037516).

3.4.5 Phosphate Buffer Saline

Phosphate buffer saline (PBS) was purchased from Pierce (Product code# 0028372). 0.15 M PBS (pH 7.4) was used for all experiments.

3.4.6 Human Serum

Filtered human serum (type# AB from male AB plasma) was purchased from Sigma Aldrich (Stock No# H4552-20ML).

3.5 Electrochemical Impedance Spectroscopy

Electrochemical impedance spectroscopy (EIS) was used to probe the protein binding event which enabled the quantitative detection of target protein CRP. EIS has seen fabulous increase in popularity in recent years with application in wide range of areas such as corrosion studies, fuel cell development, biosensors, battery health monitoring, coating performance analysis, characterization of complex electrochemical processes etc. In EIS, a small alternating potential is applied to a system and the impedance response of the system is recorded over a frequency range. Complex electrochemical systems can be modeled to an electrical equivalent circuit and the perturbation of electrode process and complex interfaces can be interrogated for studying their behavior.

Binding of target protein and their receptors in an immunoassay format on the biosensor platform can be easily probed using EIS. The PS/PANI-HCSA nanofiber surface is

functionalized with DSP linker and antiCRP is immobilized on the surface. BSA block is then applied to stop possible cross-reactivity through non-specific adsorption of non-target molecules. When target protein CRP binds with antiCRP, it essentially creates a perturbation in the electrochemical systems. Biomolecule binding at the PS/PANI-HCSA nanofiber sensor surface modulates the electrical double layer (EDL) formed at the solid-liquid interface of the analyte and the nanofiber surface. The protein binding event was probed by monitoring the capacitive layer formed at the EDL. Figure 16 shows the electrical equivalent circuit of the sensor and the schematic of the protein binding.

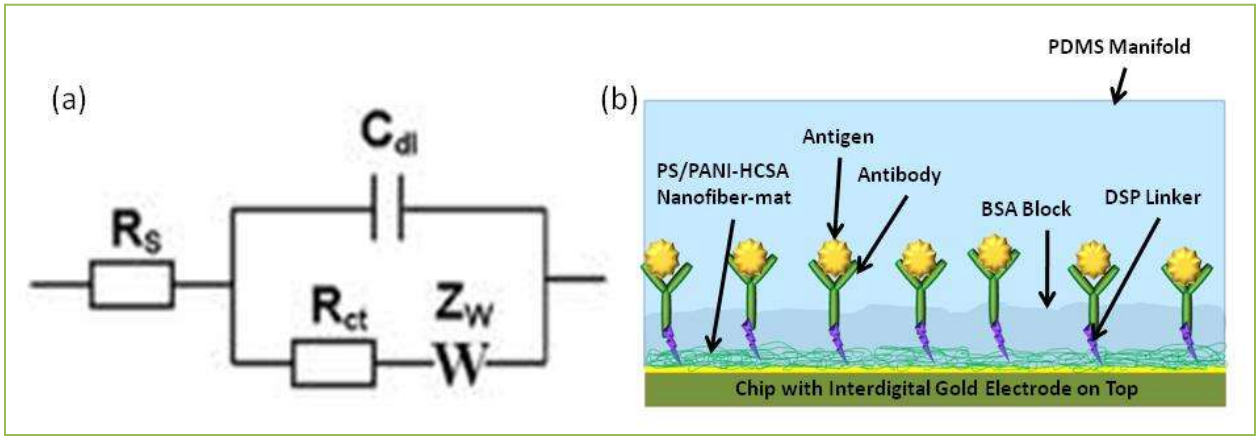

Figure 16. (a) Electrical equivalent circuit at the analyte-nanofiber interface where C_{dl} is double layer capacitance, R_{ct} is charge transfer resistance, Z_w is Warburg impedance and R_s is solution resistance, (b) schematic of protein binding event showing various components of the assay.

The electrical equivalent is based on Randell's cell model. An electrical double layer exists on the interface between the nanofiber sensor surface and the analyte. The capacitive double layer is formed as ions from the analyte forms alternating layer on the sensor surface. The binding of target protein CRP on the anti-CRP immobilized sensor surface produces a change in the double layer capacitance due to perturbation of surface charges. All charges that pass through the solution experiences the solution resistance, R_s. Some charges leak through the EDL as a

result of the electrochemical reactions at the sensor-analyte interface and these charges experience a resistance termed as charge transfer resistance, R_{ct}. Warburg impedance, Z_w is the impedance experienced by ions which diffuse from the bulk buffer to the sensor interface.

A potentiostat from Gamry Instruments (Model: Reference 600) was used for performing EIS measurements. Alternating current (AC) oscillating field of voltage amplitude 10 mV were applied and the frequency was swept from 50 Hz to 5 kHz to collect impedance response of the layered protein system. The AC fields were applied across the working and counter electrode of the microelectrode platform of the biosensor. Modulation of surface charges produces a change in C_{dl}. Frequencies only in the lower orders have been considered for this study. At these low frequencies C_{dl} undergoes major variation during antibody-antigen binding at the sensor-analyte interface. Charge transfer resistance, R_{ct} and Warburg impedance, Z_w is not dominating in these lower frequencies and mostly treated as constant. The solution resistance is also considered constant as the analyte volume is kept constant throughout the experiments. Figure 17 shows a typical impedance vs. frequency curve.

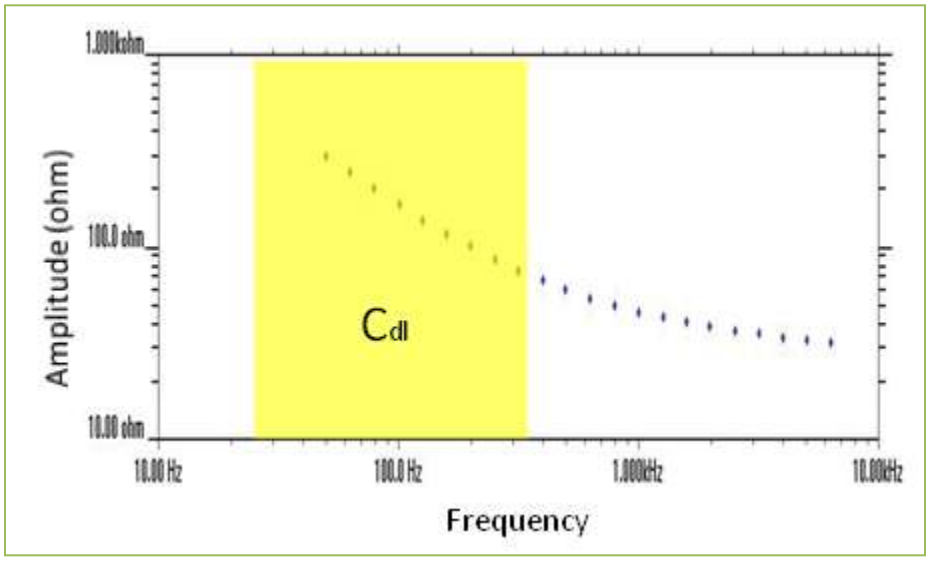

Figure 17. Typical impedance vs. frequency curve; Double layer capacitance, C_{dl} is the dominating factor at lower range of frequencies.

Since all other impedance components are not varying much at the lower range of frequencies, perturbation of C_{dl} mainly changes the impedance of the system. Therefore, the impedance measurements obtained from EIS can be directly linked to protein binding event. Higher quantity of target protein in the analyte produces higher amount of shift in the impedance from baseline and thereby allow for quantitative detection of proteins.

3.6 Experimental Protocol

All experiments followed a similar protocol for maintaining consistency. The experimental protocol is described below:

- The chip was soaked in ethanol for 15 minutes to create a contamination free device.
- The chip was then cleaned under stream of DI water for 2 minutes and air dried.
- The PS/PANI-HCSA nanofiber mat was cut in a square shape and placed on top of the gold interdigitated electrode and the PDMS manifold was attached on top using a double sided sticky tape. Caution was taken to make sure that there is no chance of leak from the manifold.
- 150 µl of 10 mM DSP was injected into the manifold to functionalize the fiber surface and prepare it for antiCRP immobilization. The chip was incubated for 30 minute at room temperature and impedance measurement was taken. Chip was then washed three times with 0.15 M phosphate buffer saline (PBS) to wash away the unbound DSP linker.
- After linker deposition, 150 µl of 50 µg/ml antiCRP was injected into the manifold and incubated for 2 hours at 4°C. Impedance measurements were taken and the sensor surface was washed three times with 0.15 M PBS.

- The block step is then performed with BSA Superblock. 150 µl of block solution is injected into the manifold and incubated for 15 minutes at room temperature. Impedance measurement was taken and the sensor surface was washed three times with 0.15 M PBS.
- Baseline measurements or zero dose measurements are performed after the block step. Either pure PBS or CRP free human serum is injected into the manifold depending upon whether the detection will be performed in buffer or human serum. Incubation period was 15 minutes at room temperature and the impedance measurement was considered as baseline measurement for that particular set of experiment. The sensor surface was washed afterwards with 0.15 M PBS.
- CRP dose response was the final step of experiment where 150 µl of CRP spiked buffer or human serum was injected into the manifold, incubated for 15 minutes and impedance measurement was taken. CRP aliquots were prepared from 1 fg/ml to 1 µg/ml concentration in a logarithmic scale either in buffer or human serum and the lowest concentration was injected in first step. After the first step, sensor surface was washed three times with 0.15 M PBS and the next highest concentration was injected and the experiment was repeated until the measurement of the highest CRP concentration was taken. Similar protocol was followed when the sensor was tested human albumin to investigate the selectivity of the device.

CHAPTER 4

RESULTS AND DISCUSSION

4.1 Fiber Architecture

Microscopic images of fibers spun at 0.5, 1.0 and 2.0 ml/hr flow rate were captured by a OLYMPUS® GX 41 Microscope and fiber diameter of electrospun fiber-mats were measured by image analysis software analySIS® FIVE. Specific surface areas of the fibers were evaluated from the measured fiber diameters. Figure 18 shows a schematic of the specific surface area calculation.

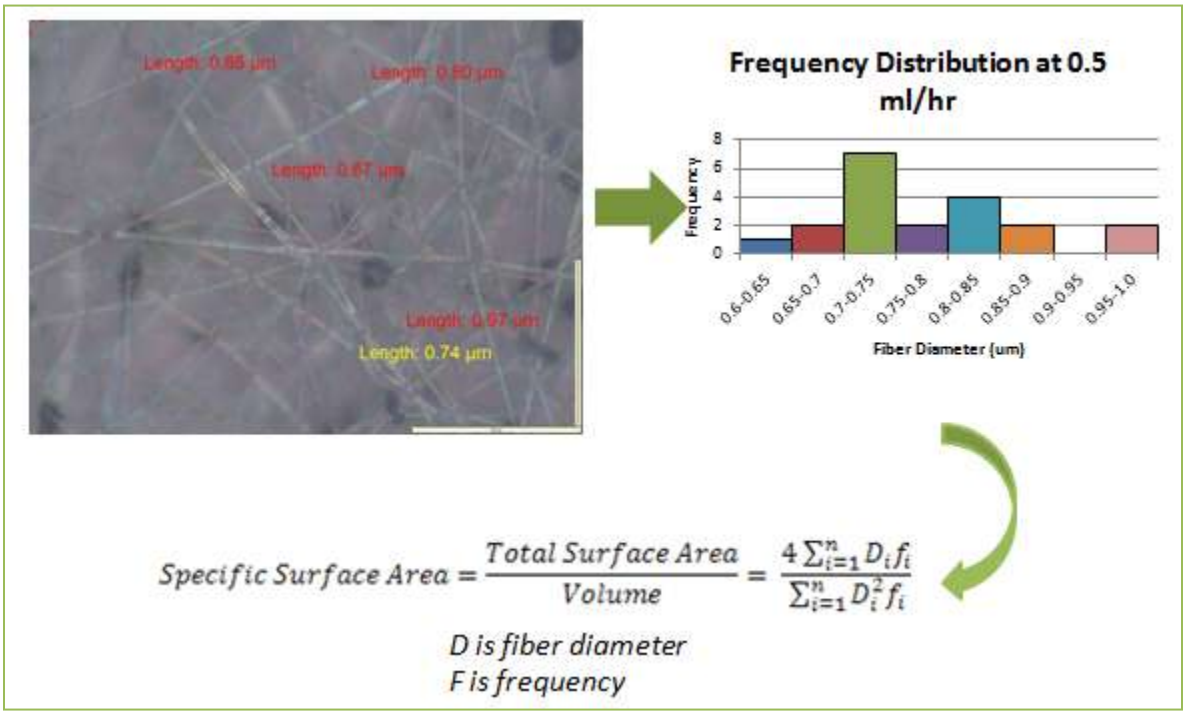

Figure 18. Schematic of specific surface area calculation. D, fiber diameter; *f*, fiber frequency; *i*, fiber number counted.

Fiber samples at different flow rate were spun on microscope slides. Microscopic images of fibers for each flow rate were captured from four random locations. Statistical fiber diameter distributions in the fiber mats were obtained. Microscopic images of the fibers at different flow

rates and graphs of statistical fiber diameter distribution are given in Appendix. Based on the fiber diameter distribution, specific surface area of fiber mat at different flow rates were calculated by equation (4.1).

$$Specific\ Surface\ Area = \frac{Total\ Surface\ Area}{Volume} = \frac{4\sum_{i=1}^{n} D_i f_i}{\sum_{i=1}^{n} D_i^2 f_i} \qquad (4.1)$$

where *D* is fiber diameter, *f* is fiber frequency and *i* is fiber number counted. Figure 19 shows the effect of flow rate on fiber diameter and specific surface area.

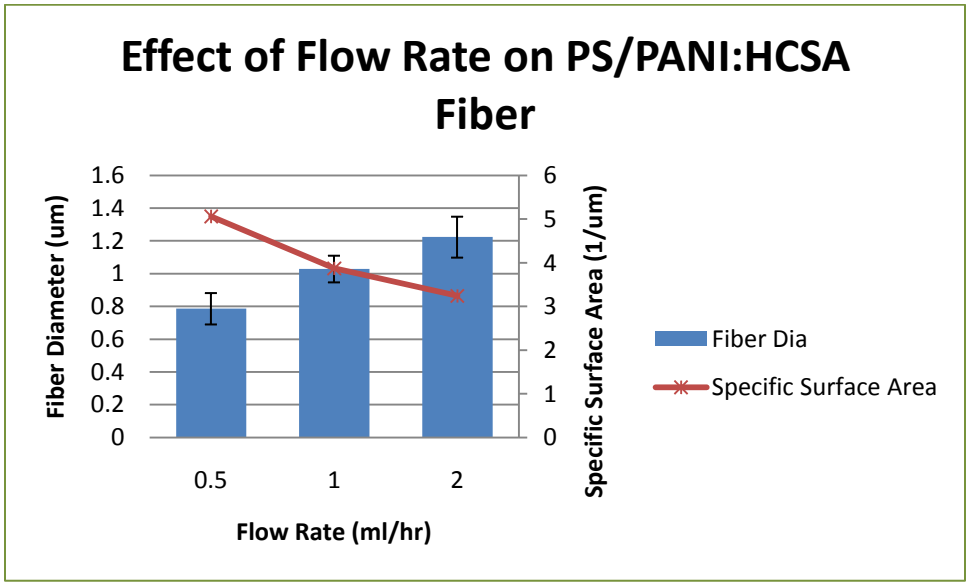

Figure 19. Graph showing effect of flow rate on fiber diameter and specific surface area.

It is evident from Figure 19 that diameter of fiber is increasing with the increase of flow rate and specific surface area is decreasing conversely. We were able to achieve mean diameter as low as 800 nm with 0.5 ml/hr flow rate. Smaller diameter of fiber provides ample parking space for the biomolecules to immobilize by increasing the specific surface area.

The efficiency of nano-fibers in increasing the specific surface area can be better understood if the specific surface area is theoretically compared with a planer film. Figure 20

shows a comparison of the specific surface area of the fiber mats and a 100 μm thick planer film with length 14.56 mm and width 14.25 mm (area of the interdigitated micro-electrode).

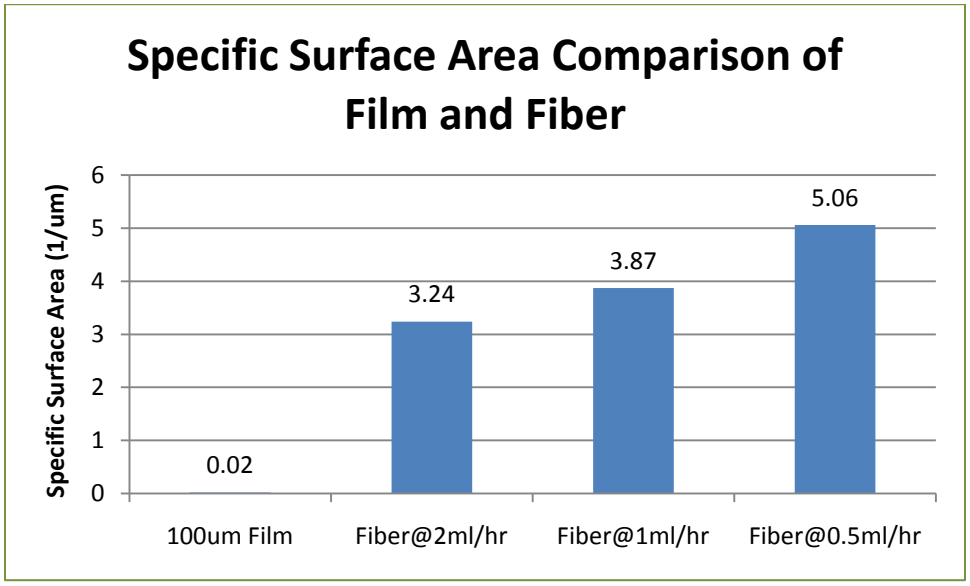

Figure 20. Comparison of specific surface area of fiber mats with a planer film.

It is apparent from Figure 20 that a planer film provides much less surface area when compared to a nano-textured fiber-mat. While trying to interpret these numbers, it has to be kept in mind that the specific surface area shown in Figure 20 is not the effective specific surface area. It is very difficult to calculate the effective specific surface area of a fiber-mat as the mat has a 3D architecture whereas the images taken by microscope are 2D. For a planer film, the effective surface area will be the area which is exposed to the analyte. Similarly the effective specific surface area of fiber mat will also decrease in reality but having fibers in the range of 1 μm will provide around 100 layers of fibers in a100 μm thick mat. This layered architecture will provide very high surface area and size matched confinements for the biomolecules to immobilize. The efficacy of fiber-mats in confining biomolecule allows the PS/PANI-HCSA fiber-mat to act as the transduction platform of our biosensor for successfully detecting CRP which will be discussed in the subsequent sections.

4.2 Sensor Performance in Buffer Saline

In this section, results showing the performance of electrospun fiber based biosensor in detecting CRP from PBS are presented. Two sets of experiments were performed to determine the sensitivity and selectivity of the sensor in buffer solution.

4.2.1 Sensitivity

The PS/PANI-HCSA nanofiber surfaces were functionalized with 10 mM DSP linker and 50 μg/ml Anti-CRP was immobilized onto the surface. After antibody immobilization the surfaces were treated with BSA blocker to block the other active sites so that non-specific binding through adsorption are minimized. Then the surfaces were washed with 150 μl of 0.15 M PBS and impedance measurements were taken over 15 minutes. These values corresponded to the baseline or zero dose measurements. A serial dilution of aliquots of CRP was prepared over a concentration ranging from 1 fg/ml to 1 μg/ml on a logarithmic scale. 150 μl of the lowest dose of CRP was injected onto the PS/PANI-HCSA surfaces and the impedance was measured after 15 minute incubation. After measuring the impedance, the sensor surface was washed with PBS and the next higher dose of CRP was injected onto the sensor surface. EIS measurements were taken at AC voltage 10 mV with a frequency sweep from 50 Hz to 5 kHz. Impedance change at 100 Hz frequency was noted for all the concentrations as the impedance at lower frequency range are mainly modulated by the protein binding event that takes place. Figure 21 shows the dose response of CRP in PBS.

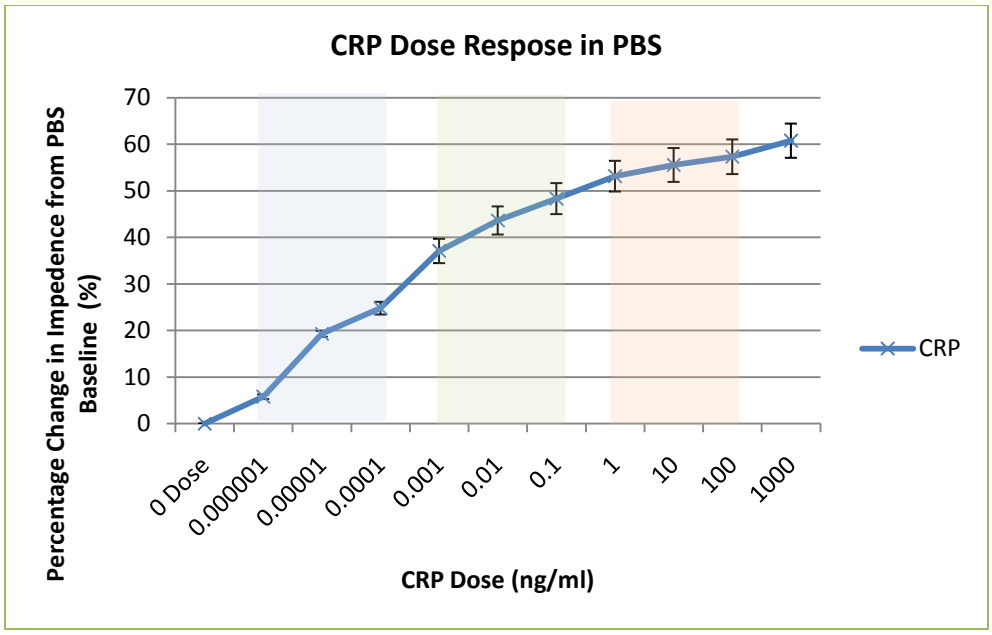

Figure 21. Dose response of C-reactive protein (CRP) in PBS on PS/PANI-HCSA nanofiber surface.

Significant change in impedance can be observed over the range of 1 fg/ml to 1 µg/ml. The percentage changes in the impedance from PBS baseline ranged from 6% to 61% on the sensor surface. Ultra low limit of detection can be observed here as the sensor is detecting CRP in femto molar regime and the dynamic range of the device is reasonably large.

4.2.2 Selectivity

To demonstrate the selectivity in detecting CRP, a competitive protein human albumin was tested on the biosensor. The chip was prepared in the same way as was done in the sensitivity experiments but albumin was used instead of CRP. Albumin aliquots were prepared in 0.15 M PBS with a serial dilution from 1 fg/ml to 1 µg/ml. Figure 22 demonstrates the selectivity of the device.

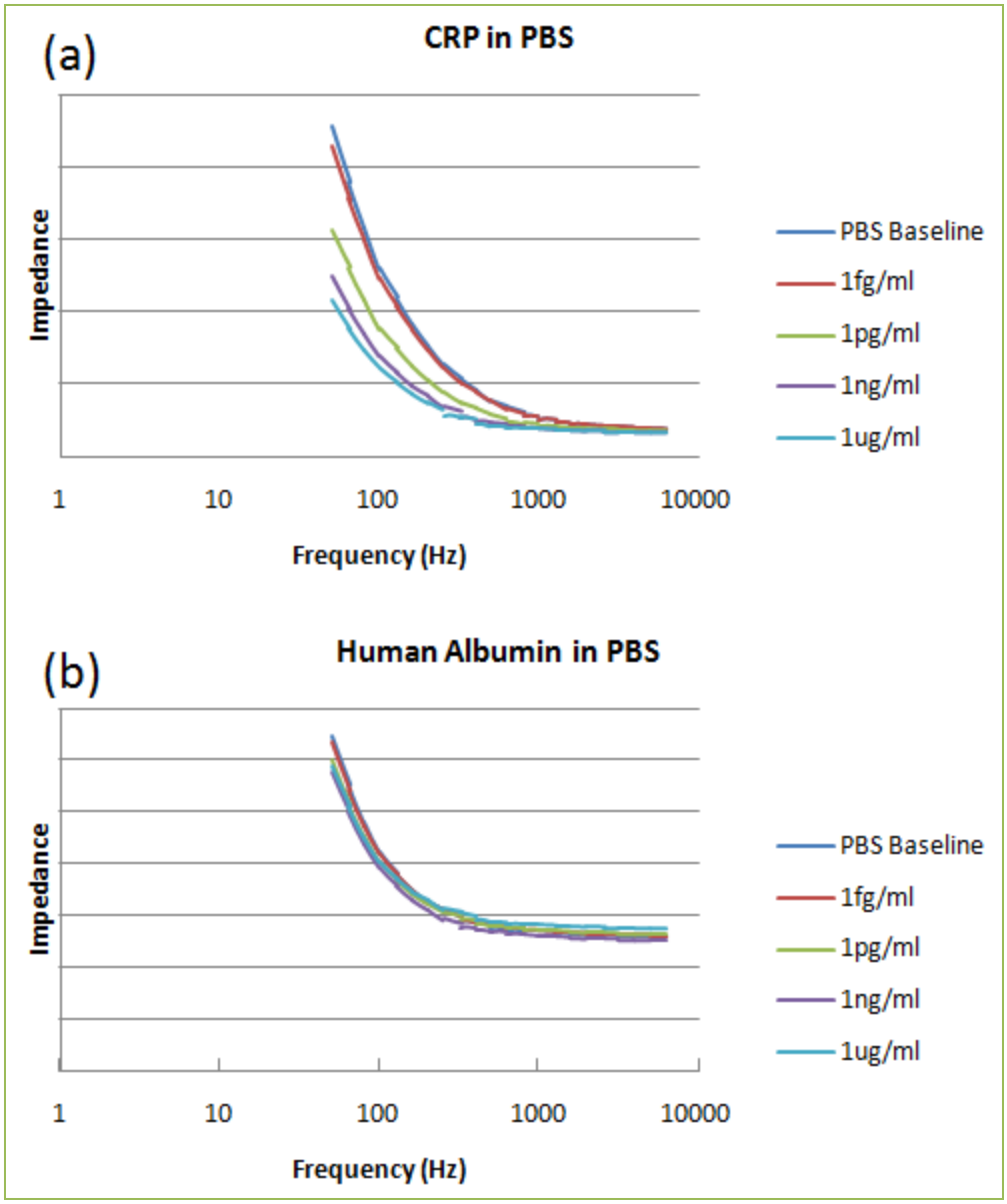

Figure 22. Comparison of impedance change of the sensor surface when exposed to (a) CRP and (b) Human Albumin.

When the target analyte CRP is injected onto the sensor surface, a clear change in the impedance at the lower frequency range is observed as the impedance can be seen going down with increasing concentration of CRP. Whereas when non-target analyte albumin is injected, impedance of the system does not change much and all the impedance curves at different concentration are clumped together. No clear trend of impedance change is visible when albumin

is injected onto the sensor surface. Figure 23 demonstrates the comparative impedance change when injected with various concentrations of CRP and Human Albumin.

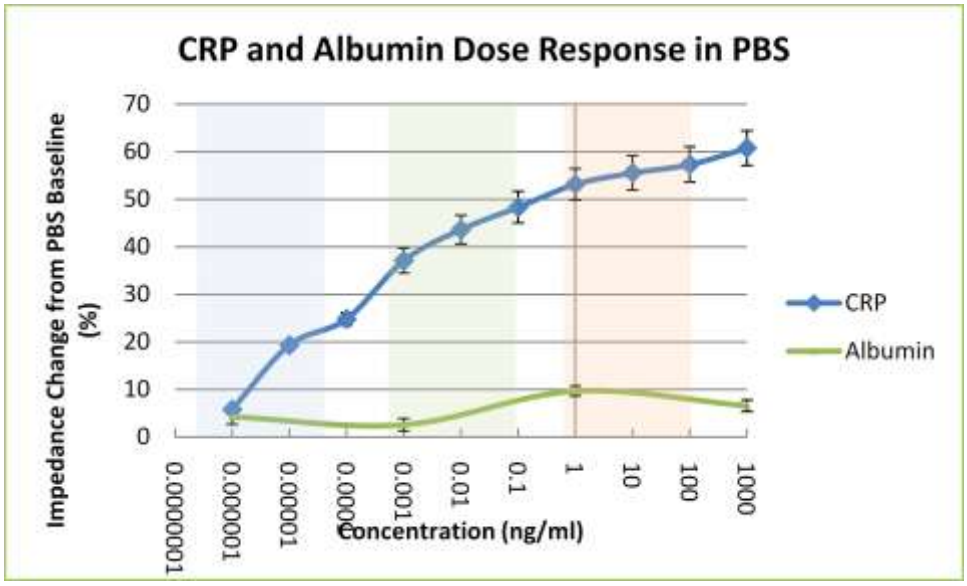

Figure 23. Dose response of CRP and Human Albumin in PBS on sensor surface.

An approximately 10% change in the impedance from the baseline PBS measurement can be observed. The graph indicates that the PS/PANI-HCSA nanofiber surface had relatively low level of cross reactivity and specifically detecting C-reactive protein from buffer solution.

4.3 Sensor Performance in Human Serum

Similar to the dose response experiments from PBS, dose response in detection of CRP from human serum was performed to identify the sensor performance in detecting CRP from complex buffers. Figure 24 shows the dose response of CRP from human serum.

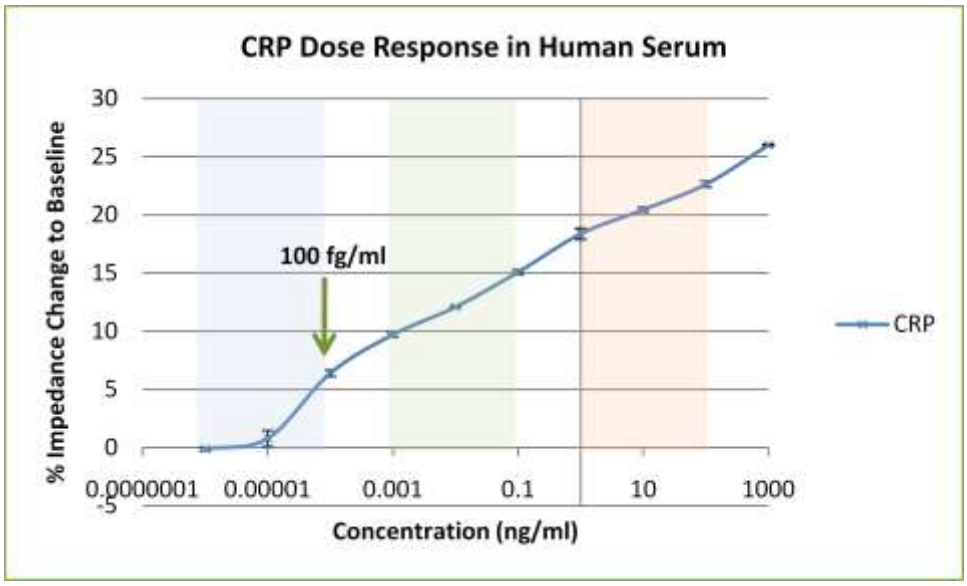

Figure 24. Dose response of C-reactive protein in commercial human serum on PS/PANI-HCSA nanofiber surface.

A change in impedance from 0 to 26% over the dose range of 1 fg/ml to 1 μg/ml of CRP in human serum from the nanofiber-mat was observed. The sensor was not able to detect CRP from human serum at 1 or 10 fg/ml concentration levels but an impedance change of 6% was observed at 100 fg/ml concentration. Although the percentage changes in impedance were lower than those observed in PBS, the changes in impedance were significant in the pico-molar and nano-molar regime and the device showed great potential to be used as a point-of-care diagnostic testing device.

4.4 Discussion

The results demonstrated in the previous sections of this chapter clearly indicate the enormous potential of this lab-on-chip platform to be used in the early detection of cardiac and inflammatory biomarkers. The experimental results have demonstrated the ability to interface nanoscale structures with micro-electrode platforms to generate a label free biosensor for protein detection. Conductive property of polyaniline was smartly utilized to generate a nano-textured surface with specific protein chemistry and protein receptors were successfully immobilized onto

the sensor surface in a repeatable fashion to ensure reliable CRP detection. CRP was detected from human serum at clinically relevant concentrations. Figure 25 shows the comparative performance of device in buffer and serum.

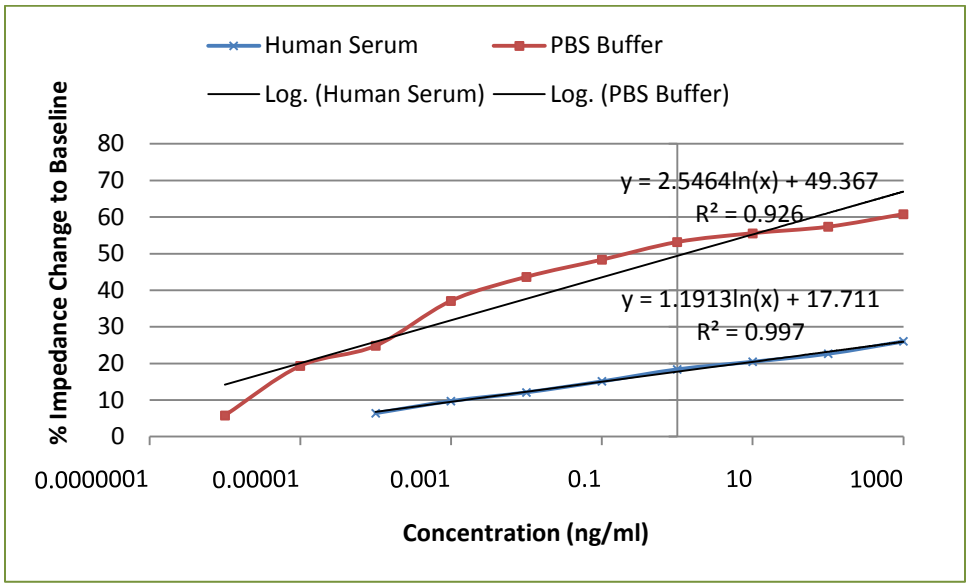

Figure 25. Comparison of sensor performance in detecting CRP from human serum and PBS.

Although impedance change achieved from human serum are much lower when compared to those from PBS, the magnitude of percentage impedance change can be considered significant to quantitatively determine CRP concentration in clinically relevant concentrations. The significant change in impedance at ultra low concentrations such as femto or pico-molar regime can be attributed to the size matching between the nanoscale compartments formed due to the layered architecture of the nanofiber mat and to the comparable size of proteins enabling protein confinement. Polyaniline enhanced the electron transduction from antibody-antigen interactions through the sensor surface allowing for near real time detection of CRP. Detection takes place in about 15 minutes and the whole assay preparation takes only about 3 hours which is extremely fast when compared with the traditional ELISA method. The volume of sample required (150 µl) can be termed as ultra-low when compared with the 3-5 ml requirement in

ELISA. A similar type of lab-on-chip platform for detecting CRP based on polystyrene/polypyrrole nanofiber was developed by Kunduru et al. [33]. Table 2 shows a comparison of the PS/PPY biosensor with PS/PANI-HCSA nanofiber based biosensor and standard ELISA assay.

TABLE 2

COMPARISON OF PS/PANI-HCSA NANOFIBER BIOSENSOR WITH ELISA AND PS/PPY NANOFIBER SENSOR

Performance Parameter	**ELISA**	**PS/PPY Nanofiber [33]**	**PS/PANI-HCSA Nanofiber**
LOD in PBS	-	1 pg/ml	1 fg/ml
LOD in Serum	100 ng/ml	No Detection (1 pg/ml in 50% diluted serum)	100 fg/ml
Linear Range of detection in PBS	-	1pg/ml-1μg/ml	1 fg/ml-1 μg/ml
Linear Range of detection in Serum	100 ng/ml-100 μg/ml	No Detection (1 pg/ml in 50% diluted serum)	100 fg/ml-1 μg/ml
Sample Volume	3-5 ml	150 μl	150 μl
Assay Time	> 24 hrs	3 hrs	3 hrs
Detection Method	Enzyme linked immunoassay	Label free impedance	Label free impedance

Table 2 clearly demonstrates the excellent performance of PS/PANI-HCSA nanofiber based sensor in terms of limit of detection, dynamic range, sample volume required and assay preparation time.

4.5 Limitations

Although this device holds great promise to be developed as a portable label free lab-on-chip platform, it is not free from its limitations. Lack of control over the fiber architecture is inherent limitation of electrospun fiber mat and this issue has to be addressed by performing

large set of experiments to have a strong statistical base. The sensor surface is not reusable and thus viability of making this into a disposable chip has to be considered or an efficient method of replacing the nanofiber sensor surface has to be developed. Polyaniline is known to lose its conducting property over time when exposed to air and therefore long term stability of the device is an issue that has to be studied. Cross-reactivity with competing protein in human serum is not tested so far. Extensive study has to be done to determine cross-reactivity with competing protein in human serum and ensure selectivity of the device.

CHAPTER 5

CONCLUSION AND FUTURE WORK

Ability to utilize the conductive properties of polyaniline in developing an ultrasensitive immunosensor for cardiovascular risk biomarker has been demonstrated in this project. Electrspun fiber from PS/PANI-HCSA has been produced with nanoscale architecture and used as the sensing element on a lab-on-chip platform. Results indicate that high specific surface area and porous architecture of nanofiber makes it an ideal candidate for biosensor sensing element. CRP was successfully detected at 100 fg/ml concentration from human serum suggesting the potential of this lab-on-chip platform for early detection of any cardiovascular risk. It has been demonstrated that scaling down to nanotextured architecture helps in creating size matched confinement which enhances the sensitivity of this detection method. A large dynamic linear range of 100 fg/ml-1 μg/ml was achieved in human serum for detection of CRP. Less than 10% cross-reactivity with human albumin suggests the selective detection capability of the proposed biosensor.

The transition of a laboratory scale idea into a marketable product is a massive challenge. Extensive study on selectivity of proposed biosensor platform has to be carried out to ensure selective detection of target biomolecule in a more competitive environment. Long term stability of the sensing element has to be experimentally investigated to ensure dependable device performance. The chip has to be integrated with a small electronic measurement and readout system for this idea to transform into a product. None the less, the success of this project opens up an enchanting avenue for possible future work. Detailed study on the optimization of process parameters for electrospinning PS/PANI-HCSA nanofiber can be conducted and the effect of varying fiber morphology on sensor performance can be investigated. Effect of blending

polyaniline with other polymers and their performance as biosensor can be investigated. Addition of nanomaterials such as carbon nanotube or gold nanoparticle into electrospun fiber can be a very interesting area of sensor research. Nanomaterial inclusions can act as hot spots for biomolecule binding and increase the sensitivity of sensor. Another interesting challenge would be designing an electrospun fiber based lab-on-chip platform with capability of detecting multiple disease biomarkers simultaneously. Nanotechnology is growing everyday and holds enormous potential. Future belongs to the so called bottom-up technologies and biosensor technology will keep on growing along the way.

REFERENCES

REFERENCES

[1] Formhals, A., "Process and Apparatus for Preparing Artificial Threads." *US Patent 1975504*, 1934.

[2] Ikegame, M., Tajima, K. and Aida, T., "Template Synthesis of Polypyrrole Nanofibers Insulated Within One-Dimensional Silicate Channels: Hexagonal Versus Lamellar for Recombination of Polarons into Bipolarons." *Angewandte Chemie International Edition*, Vol. 42, No. 19, 2003, pp. 2154-57.

[3] Martin, C. R., "Membrane-Based Synthesis of Nanomaterials." *Chemistry of Materials*, Vol. 8, 1996, pp. 1739-46.

[4] Ondarcuhu, T. and Joachim, C., "Drawing a Single Nanofibre over Hundreds of Microns." *Europhysics Letter*, Vol. 42, No. 2, 1998, pp. 215-20.

[5] Feng, X., Yang, G., Xu, Q., Hou, W. and Zhu, Z., "Self-Assembly of Polyaniline/Au Composites: from Nanotubes to Nanofibers." *Macromolecular Rapid Communications*, Vol. 27, No. 1, 2006, pp. 31-36.

[6] Yang, Z. and Xu, B., "Supramolecular Hydrogels based on Biofunctional Nanofibers of Self-assembled Small Molecules." *Journal of Materials Chemistry*, Vol. 17, 2007, pp. 2385-93.

[7] Ma, P., X., and Zhang, R., "Synthetic Nano-scale Fibrous Extracellular Matrix." *Journal of Biomedical Materials Research Part A*, Vol. 46, No. 1, 1999, pp. 60-72.

[8] Ellison, C., J., Phatak, A., Giles, D., W., Macosko, C., W. and Bates, F., S., "Melt Blown Nanofibers: Fiber Diameter Distributions and Onset of Fiber Breakup." *Polymer*, Vol. 48, 2007, pp. 3306-16.

[9] Ramakrishna, S., Fujihara, K., Teo, W., Lim, T. and Ma, Z., *An Introduction to Electrospinning and Nanofibers*, World Scientific Publishing Co. Pte. Ltd., Singapore, 2005.

[10] Taylor, G., I., "Electrically Driven Jets." *Proceedings of Royal Society of London*, Vol. 313, 1969, pp. 453-75.

[11] Taylor, G., I. and McEwan, A., D., "The Stability of Horizontal Fluid Interface in a Vertical Electric Field." *Journal of Fluid Mechanics*, Vol. 22, No. 1, 1965, pp. 1-15.

[12] Reneker, D., H., Yarin, A., L., Fong, H. and Koombhongse, S., "Bending Instability of Electrically Charged Liquid Jets of Polymer Solutions in Electrospinning." *Journal of Applied Physics*, Vol. 87, No. 9, 2000, pp. 4531-47.

[13] Hohman, M., M., Shin, M., Rutledge, G. and Brenner, M., P., "Electrospinning and Electrically Forced Jets. I. Stability Theory." *Physics of Fluids*, Vol. 13, No. 8, 2001,pp. 2201-20.

[14] Hohman, M., M., Shin, M., Rutledge, G. and Brenner, M., P., "Electrospinning and Electrically Forced Jets. II. Applications." *Physics of Fluids*, Vol. 13, No. 8, 2001,pp. 2221-36.

[15] Jiang, H., L., Fang, D., F., Hsiao, B., S., Chu, B. and Chen,W., "Optimization and characterization of dextran membranes prepared by electrospinning." *Biomacromolecules*, Vol. 5, No. 2, 2004, pp. 326-333.

[16] Mit-uppatham, C., Nithitanakul, M., and Supaphol, P., "Ultrafine Electrospun Polyamide-6 Fibers: Effect of Solution Conditions on Morphology and Average Fiber Diameter." *Macromolecular Chemistry and Physics*, Vol. 205, No. 17, 2004, pp. 2327-38.

[17] Zong, X., Kim, K., Fang, D., Ran, S., Hsiao, B., S. and Chu, B., "Structure and Process Relationship of Electrospun Bioabsorbable Nanofiber Membranes." *Polymer*, Vol. 43, No. 16, 2002, pp. 4403-12.

[18] Deitzel, J., M., Kleinmeyer, J., Harris, D. and Tan, N., C., B., "The Effect of Processing Variables on the Morphology of Electrospun Nanofibers and Textiles." *Polymer*, Vol. 42, No. 1, 2001, pp. 261-72.

[19] Huang, L., Nagapudi, K., Apkarian, R., P. and Chaikof, E., L., "Engineered collagen–PEO nanofibers and fabrics." *Journal of Biomaterial Science: Polymer Edition*, Vol. 12, No. 9, 2001, pp. 979-93.

[20] Son, W., K., Youk, J., H., Lee, T., S. and Park, W. H., "The Effects of Solution Properties and Polyelectrolyte on Electrospinning of Ultrafine Poly(Ethylene Oxide) Fibers." *Polymer*, Vol. 45, No. 9, 2004, 2959-66.

[21] Krisnappa, R., V., N., Desai, K. and Sung, C., "Morphological Study of Electrospun Polycarbonates as a Function of the Solvent and Processing Voltage." *Journal of Material Science*, Vol. 38, 2003, pp. 2357-65.

[22] Zhang, C., Yuan, X., Wu, L., Han, Y. and Sheng, J., "Study on Morphology of Electrospun Poly(Vinyl Alcohol) Mats." *European Polymer Journal*, Vol. 41, No. 3, 2005, pp. 423-32.

[23] Mo, X., M., Xu, C., Y., Kotaki, M. and Ramkrishna, S., "Electrospun P(LLA-CL) Nanofiber: A Biomimetic Extracellular Matrix for Smooth Muscle Cell and Endothelial Cell Proliferation." *Biomaterials*, Vol. 25, No. 10, 2004, pp. 1883-90.

[24] Liu, H. and Hsieh, Y., "Ultrafine Fibrous Cellulose Membranes from Electrospinning of Cellulose Acetate." *Journal of Polymer Science Part B: polymer Physics*, Vol. 40, No. 18, 2002, pp. 2119-29.

[25] Casper, C., L., Stephens, J., S., Tassi, N., G., Chase, B. and rabolt, J., F., "Controlling Surface Morphology of Electrospun Polystyrene Fibers: Effect of Humidity and Molecular Weight in the Electrospinning Process." Macromolecules, Vol. 37, No. 2, 2004, pp. 573-78.

[26] Pham, Q., P., Sharma, U. and Mikos, A., G., "Electrospinning of Polymeric Nanofibers for Tissue Engineering Applications: A Review." Tissue Engineering, Vol. 12, no. 5, 2006, pp. 1197-1211.

[27] Aussawasathien, D., Dong, J., H. and Dai, L., "Electrospun Polymer Nanofiber Sensor." *Synthetic Metals*, Vol. 154, 2005, pp. 37-40.

[28] Pinto, N., J., Johnson, A., T., MacDiarmid, A., G., Mueller, C., H., Theofylaktos, N., Robinson, D., C. and Miranda, F., A., "Electrospun polyaniline/polyethylene oxide nanofiber field-effect transistor." *Applied Physics Letters*, Vol. 83, No. 20, 2003, pp. 4244-47.

[29] Sawicka, K., Gouma, P. and Simon, S., "Electrospun Biocomposite Nanofibers for Urea Biosensing." *Sensors and Actuators B: Chemical*, Vol. 108, No. 1-2, 2005, pp. 585-88.

[30] Bishop, A. and Gouma, P., "Leuco-emeraldine based Polyaniline-Poly-vinyl-pyrrolidone Electrospun Composites and Bio-composites: A Preliminary Study of Sensing Behavior." *Review on Advance Material Science*, Vol. 10, 2005, pp. 209-14.

[31] Wang, G., Ji, Y., Huang, X., Yang, X., Gouma, P. and Dudley, M., "Fabrication and Characterization of Polycrystalline WO_3 Nanofibers and Their Application for Ammonia Sensing." *The Journal of Physical Chemistry B*, Vol. 110, No. 47, 2006, pp. 23777-82.

[32] Wang, X., Kim, Y., Drew, C., Ku, B., Kumar, J. and Samuleson, L., A., "Electrostatic Assembly of Conjugated Polymer Thin Layers on Electrospun Nanofibrous Membranes for Biosensors." *Nano Letters*, Vol, 4, No. 2, 2004, pp. 331-34.

[33] Kunduru, V., Bothara, M., Grosch, J., Sengupta, S., Patra, P., K. and Prashad, S., "Nanostructured Surface for Enhanced Protein Detection Toward Clinical Diagnostics." *Nanomedicine: NBM*, Vol. 6, No. 5, 2010, pp. 642-50.

[34] Li, S., Floriano, P., N., Christodoulides, N., Fozdar, D., Y., Shao, D., Ali, M., F., Dharshan, P., Mohanty, S., Neikirk, D., Mcdevitt, J., T. and Chen, S., "Disposable Polydimethylsiloxane/Silicon Hybrid Chips for Protein Detection." *Biosensors and Bioelectronics*, Vol. 21, No. 4, 2005, pp. 574-80.

[35] Lin, H., Y., Tseng, K., Y., Hu, W., P., Hsu, H., Y., Chiou, A., Chang, G., L. and Chen, S., "Direct Detection of C-reactive Protein in Human Serum Using Nanoparticle Enhanced Surface Plasmon Resonance Biosensing." *Proceedings of SPIE*, Vol. 6324, 2006, pp. 1-11.

[36] Bhattacharyya, A. and Klapperich, C., M., "Design and Testing of a Disposable Microfluidic Chemiluminescent Immunoassay for Disease Biomarkers in Human Serum Samples." *Biomedical Microdevices*, Vol. 9, No. 2, 2007, pp. 245-51.

[37] Bini, A., Centi, S., Tombelli, S., Minunni, M. and Mascini, M., "Development of an Optical RNA-based Aptasensor for C-reactive Protein." *Analytical and Bioanlytical Chemistry*, Vol. 390, No. 4, 2008, pp. 1077-86.

[38] Kim, D., K., Kerman, K., Yamamura, S., Kwon, Y., S., Takamura, Y. and Tamiya, E., "Label Free Optical Detection of Protein Antibody-Antigen Interaction on Au Capped Porous Anodic Alumina Layer Chip." *Japanese Journal of Applied Physics*, Vol. 47, No. 2, 2008, pp. 1351-54.

[39] Kim, H., C., Lee, S., K., Jeon, W., B., Lyu, H., Lee, S., W. and Jeong, S., W., "Detection of C-reactive Protein on a Functional Poly(thiophene) Self-assembled Monolayer Using Surface Plasmon Resonance." *Ultramicroscopy*, Vol. 108, No. 10, 2008, pp. 1379-83.

[40] Padigi, S., K., Asante, K., Kovvuri, V., S., R., Reddy, R., K., K., Rosa, A., L. and Prasad, S., "Micro-photonic Cylindrical Waveguide Based Protein Biosensor." *Nanotechnology*, Vol. 17, 2006, pp. 4384-90.

[41] Fournet, M., E., B., Ledwith, D., Voisin, M., Cunningham, S. and Fournet, P., "High Surface Plasmon Resonant Sensitive Silver Nanoplates for Detection of C-reactive Protein." *IEEE Conference on Nanotechnology*, Genoa, 2009, pp. 866-69.

[42] Lee, W., B., Chen, Y. H., Lin, H., Huang, C., J., Shiesh, S., C. and Lee, G., B., "A Microfluidic System Integrated With Optical Detection Devices for Automatic Detection of C-reactive Protein." *IEEE International Conference on Micro Electro Mechanical Systems*, Hong Kong, 2010, pp. 979-82.

[43] Gul, O., Kallempudi, S., S., Basaga, H., Sezerman, U. and Gurbuz, Y., "Biosensor for the Detection of Cardiovascular Risk Markers in Human Serum." *PRIME: 2008 PhD Research in Microelectronics and Electronics Proceedings*, Istanbul, Turkey, 2008.

[44] Quershi, A., Gurbuz, Y., Kang, W., P. and Davidson, J., L., "A Novel Interdigitated Capacitor Based Biosensor for Detection of Cardiovascular Risk Biomarker." *Biosensors and Bioelectronics*, Vol. 25, No. 4, 2009, pp. 877-82.

[45] Quershi, A., Gurbuz, Y., Howell, M., Kang, W., P. and Davidson, J., L., "Nanocrystalline Diamond Film for Biosensor Applications." *Diamond and Related Materials*, vol. 19, No. 5-6, 2010, pp. 457-61.

[46] Kunduru, V. and Prasad, S., "Electrokinetic Formation of "Microbridges" for Protein Biomarkers as Sensors." *Journal of the Association for Laboratory Automation*, Vol. 12, No. 5, 2007, pp. 311-17.

[47] Bothara, M., G., Reddy, R., K., Barrett, T., Carruthers, J. and Prasad, S., "Nanoporous Alumina Membranes Based Microdevices for Ultrasensitive Protein Detection." *Technical Proceedings of the 2008 NSTI Nanotechnology Conference and Trade Show*, Boston, 2008, pp. 344-47.

[48] Lin, K., C., Kunduru, V., Bothara, M., Rege, K., Prasad, S. and Ramkrishna, B., L., "Biogenic Nanoporous Silica-based Sensor for Enhanced Electrochemical Detection of Cardiovascular Biomarkers Proteins." *Biosensors and Bioelectronics*, Vol. 25, No. 10, 2010, pp. 2336-42.

[49] Sohn, Y., S. and Kim, Y., T., "Field-effect-transistor Type C-reactive Protein Sensor using Cysteine-tagged Protein G." *Electronic Letters*, Vol. 44, No. 16, 2008, pp. 955-56.

[50] Singh, K., V., Whited, A., M., Ragineni, Y., Barrett, T., W., King, J. and Solanki, R., "3D Nanogap Interdigitated Electrode Array Biosensors." *Analytical and Bioanalytical Chemistry*, Vol. 397, No. 4, 2010, pp. 1493-1502.

[51] Lee, M., H., Lee, K., N., Jung, S., W., Kim, W., H., Shin, K., S. and Seong, W., K., "Quantitative Measurements of C-reactive Protein Using Silicon Nanowire Array." *International Journal of Nanomedicine*, Vol. 3, No. 1, 2008, pp. 117-24.

[52] Qureshi, A., Gurbuz, Y. and Niazi, J., H., "Label free Detection of cardiac Biomarker Using Aptamer Based Capacitive Biosensor." *Procedia Engineering*, Vol. 5, 2010, pp. 828-30.

[53] Qureshi, A., Gurbuz, Y., Kallempudi, S. and Niazi, J., H., "Label-free RNA Aptamer-based Capacitive Biosensor for the Detection of C-reactive Protein." *Physical Chemistry Chemical Physics*, Vol. 12, 2010, pp. 9176-82.

[54] Wee, K., W., Kang, G., Y., Park, J., Kang, J., Y., Yoon, D., S., Park, J., H. and Kim, T., S., "Novel Electrical Detection of Label-free Disease Marker Proteins Using Piezoresistive Self-sensing Micro-cantilevers." *Biosensors and Bioelectronics*, Vol. 20, No. 10, 2005, pp. 1932-38.

[55] Chen, C., H., Hwang, R., Z., Huang, L., S., Lin, S., M., Chen, H., C., Yang, Y., C., Lin, Y., T., Yu, S., A., Lin, Y., S., Wang, Y., H., Chou, N., K. and Lu, S., S., "A Wireless BioMEMS Sensor for C-reactive protein Detection based on Nanomechanics." *IEEE Transactions on Biomedical Engineering*, Vol. 56, No. 2, 2009, pp. 462-70.

[56] McBride, J., D. and Cooper, M., A., "A High Sensitivity Assay for the Inflammatory Marker C-Reactive Protein Employing Acoustic biosensing." *Journal of Nanobiotechnology*, Vol. 6, No. 1, 2008, pp. 5-13.

[57] Yatsuda, H., Kogai, T., Goto, M., Chard, M. and Athey, D., "Biosensor Using Shear-Horizontal Surface Acoustic Wave." *Microwave Conference Proceedings*, Hangzhou, China, 2011, pp. 1-4.

[58] Black, S., Kushner, I. and Samols, D., "C-reactive Protein." *The Journal of Biological Chemistry*, Vol. 279, No. 47, 2004, pp. 48487-90.

[59] Agrawal, A. and Volanakis, J., E., "Probing the C1q-binding Site on Human C-reactive Protein by Site-directed mutagenesis." *The Journal of Immunology*, Vol. 152,No. 11, 1994, pp. 5404-10.

[60] Ridker, P., M., "Clinical Application of C-Reactive Protein for Cardiovascular Disease Detection and Prevention." *Journal of the American Heart Association*, Vol. 107, 2003, pp. 363-69.

[61] Pradhan, A., D., Manson, J., E., Rifai, N., Buring, J., E. and Ridker, P., M., "C-Reactive Protein, Interleukin 6, and Risk of Developing Type 2 Diabetes Mellitus." Journal of American Medical Association, Vol. 286, No. 3, 2001, pp. 327-34.

APPENDIX

APPENDIX

MICROSCOPIC IMAGES OF ELECTROSPUN FIBER AND FIBER DIAMETER DISTRIBUTION AT DIFFERENT FLOW RATES

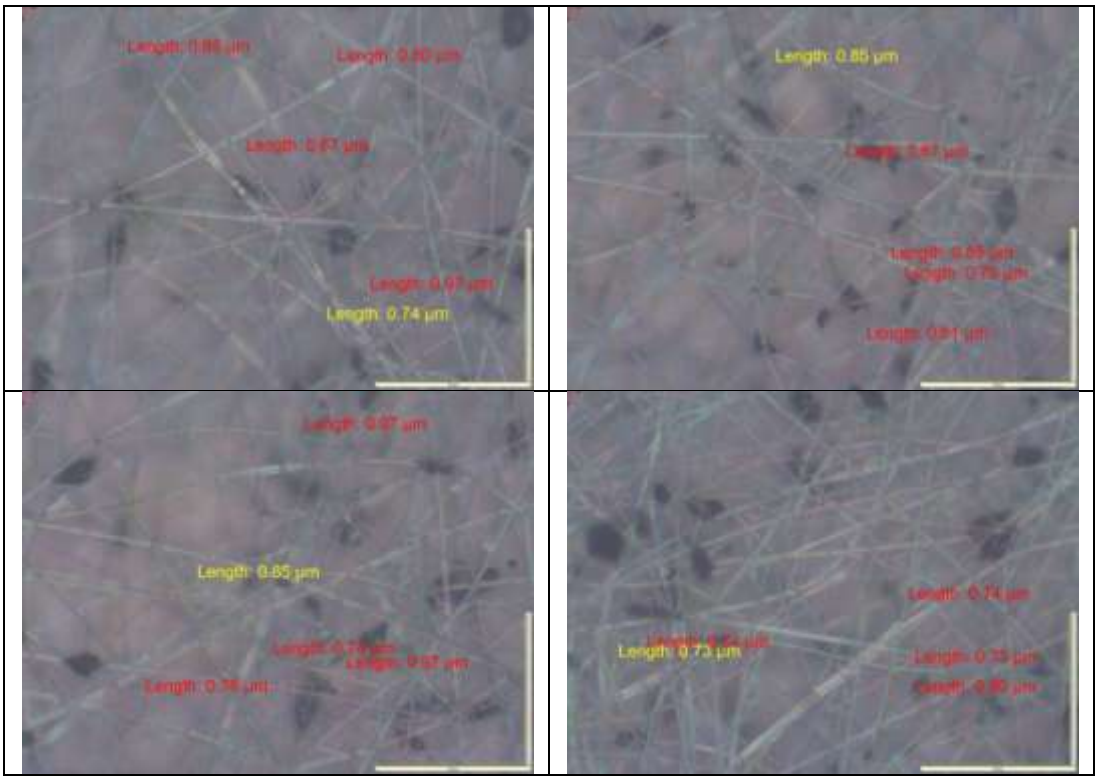

Figure 1: Microscopic images of fibers taken at 4 random locations when the fiber was electrospun at 0.5 ml/hr flow rate

.

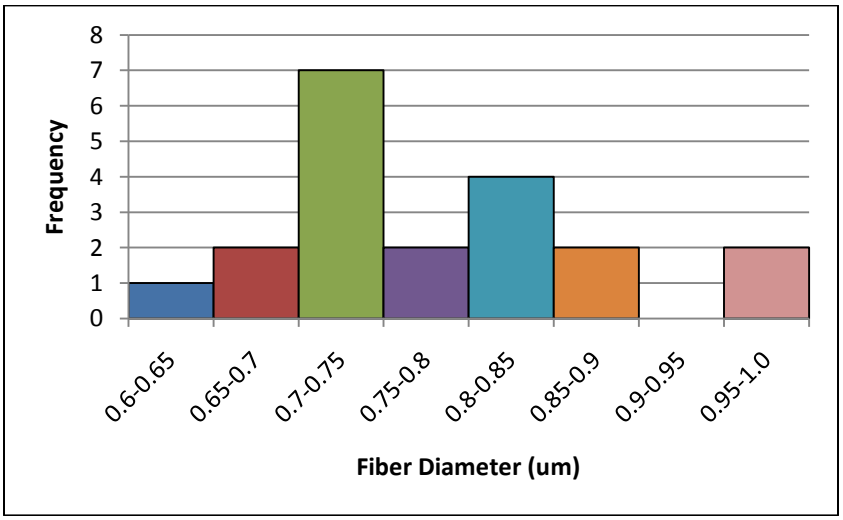

Figure 2: Fiber diameter distribution calculated for fibers spun at 0.5 ml/hr flow rate.

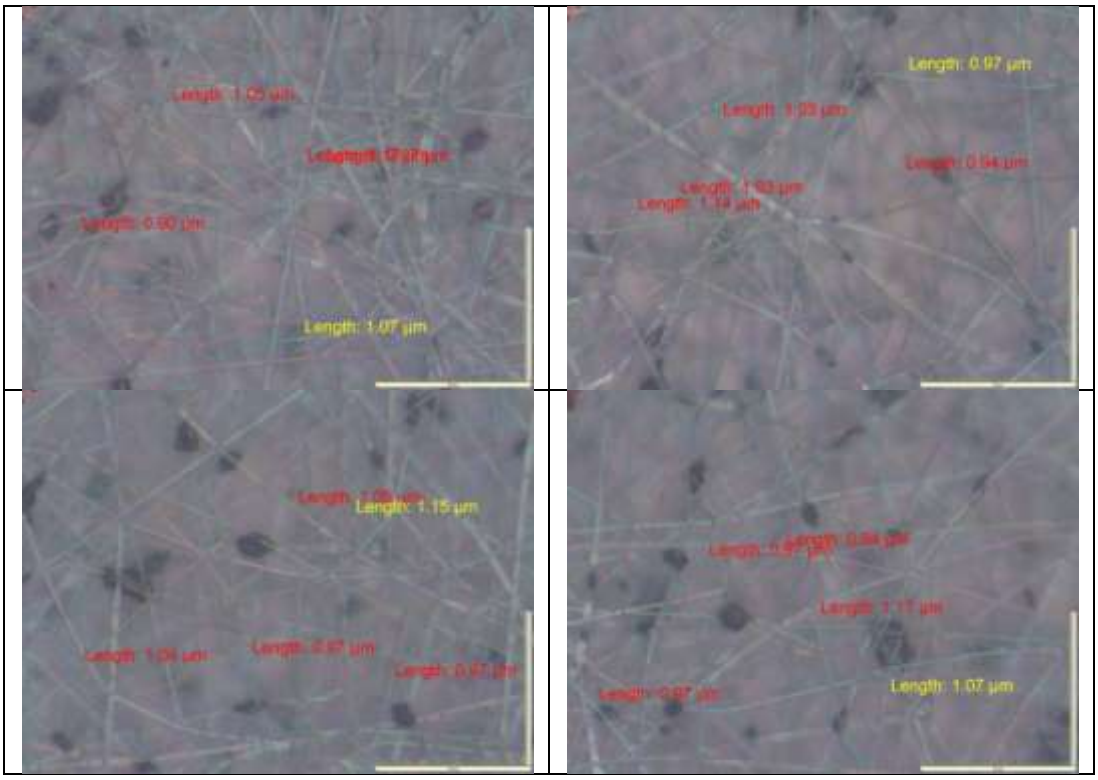

Figure 3: Microscopic images of fibers taken at 4 random locations when the fiber was electrospun at 1 ml/hr flow rate

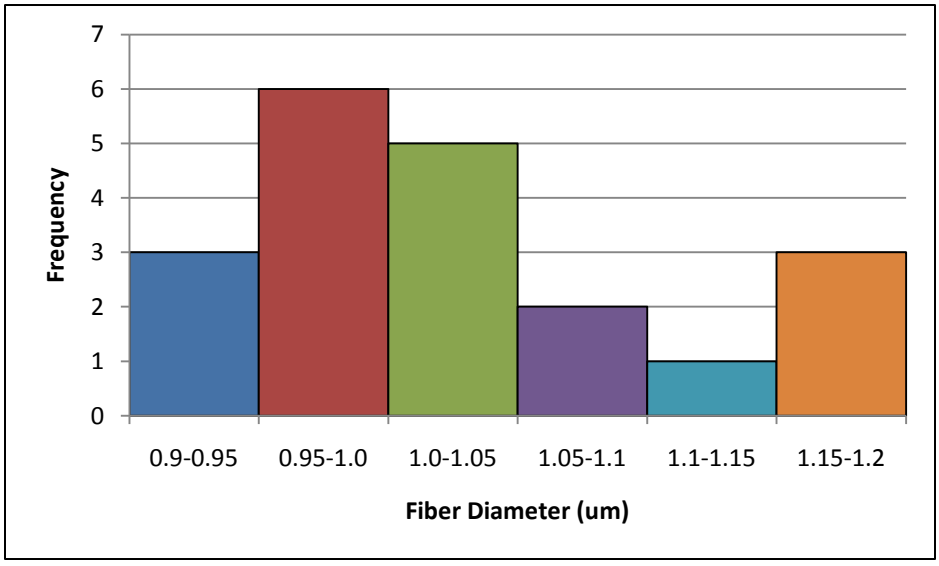

Figure 4: Fiber diameter distribution calculated for fibers spun at 0.5 ml/hr flow rate.

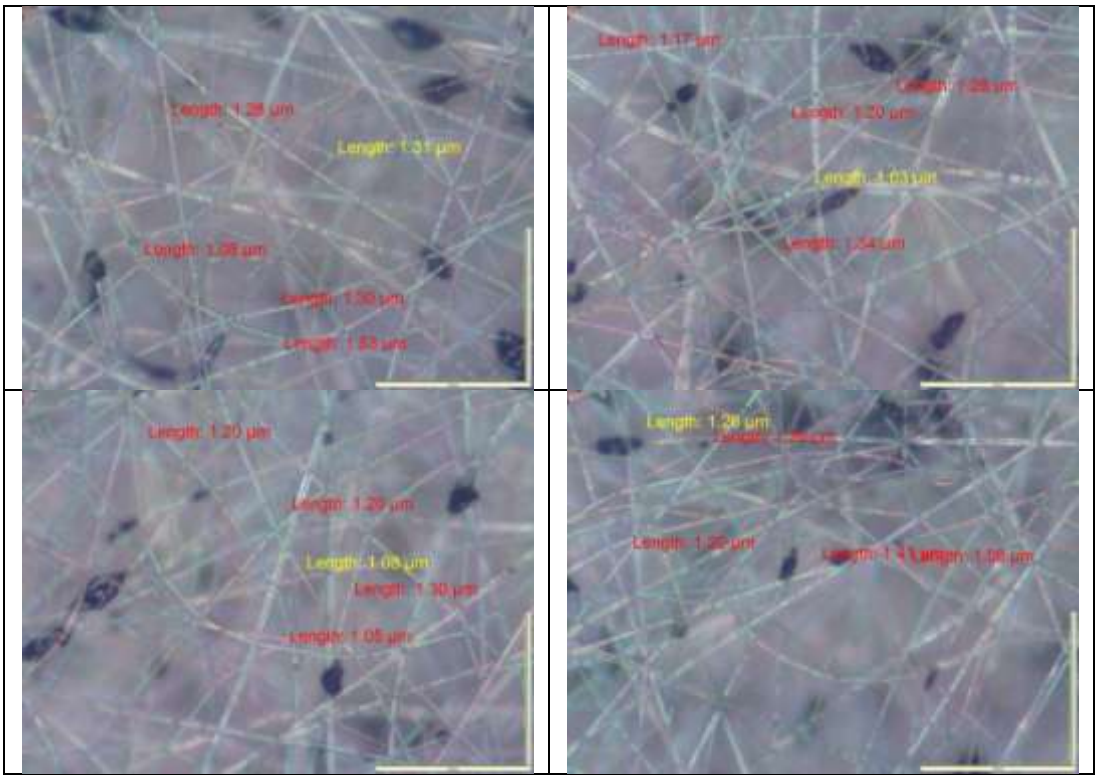

Figure 5: Microscopic images of fibers taken at 4 random locations when the fiber was electrospun at 2 ml/hr flow rate

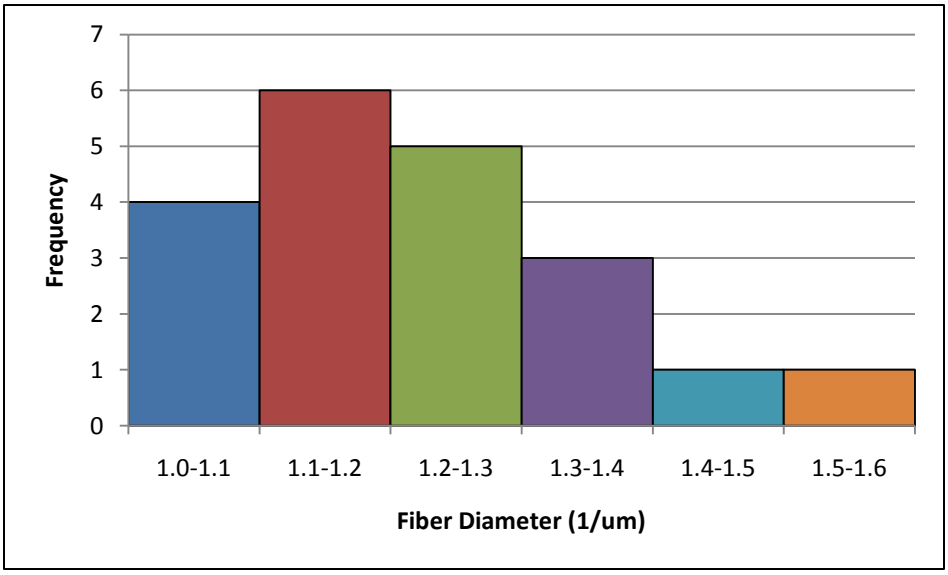

Figure 6: Fiber diameter distribution calculated for fibers spun at 2 ml/hr flow rate.